DIETARY PROTECTION AGAINST THE VISUAL AND MOTOR DEFICITS INDUCED BY EXPERIMENTAL AUTOIMMUNE ENCEPHALOMYELITIS

Katarzyna Zyla-Jackson[1,2], Dorothy A. Walton[1], Kendra S. Plafker[1], Susan Kovats[3], Constantin Georgescu[4], Richard S. Brush[5], Madison Tytanic[5], Martin-Paul Agbaga[2,5], and Scott M. Plafker[1,2,*]

[1]*Aging and Metabolism Research Program, Oklahoma Medical Research Foundation, Oklahoma City, USA*
[2]*Department of Cell Biology, University of Oklahoma Health Sciences Center, Oklahoma City, USA*
[3]*Arthritis and Clinical Immunology Research Program, Oklahoma Medical Research Foundation, Oklahoma City, USA and Dept of Microbiology and Immunology University of Oklahoma Health Sciences Center, Oklahoma City, USA*
[4]*Genes and Human Disease Research Program, Oklahoma Medical Research Foundation, Oklahoma City, USA*
[5]*Dean McGee Eye Institute, University of Oklahoma Health Sciences Center, Oklahoma City, USA*

[*] Corresponding author:
Scott M Plafker, Aging and Metabolism Research Program, Oklahoma Medical Research Foundation, 825 NE 13th St, OKC, OK, 73104.
Email: plafkers@omrf.org

Keywords
Optic neuritis, multiple sclerosis, optic nerve, retinal ganglion cells, experimental autoimmune encephalomyelitis, ketogenic diet

ABSTRACT

5-8% of the world population currently suffers from at least one autoimmune disorder. Despite multiple immune modulatory therapies for autoimmune demyelinating diseases of the CNS, these treatments are restricted to subsets of patients. To overcome these barriers, we investigated a nutritional intervention in mice undergoing experimental autoimmune encephalomyelitis (EAE). This model of autoimmune-mediated demyelination induces visual and motor pathologies similar to those experienced by patients with multiple sclerosis. Here, we report that limiting dietary carbohydrates by feeding mice a well-formulated ketogenic diet (WFKD) enriched in medium chain triglycerides, α-linolenic acid, and fiber protects from EAE-induced optic neuritis and motor deficits. The WFKD increased circulating ketones but did not cause weight gain while preserving visual acuity and motor function in both female and male EAE mice. Immunohistochemistry of optic nerves revealed that the WFKD preserved oligodendrocytes and reduced infiltrating T cells and macrophages. The WFKD also increased anti-inflammatory-associated omega-3 fatty acids in the plasma and reduced select cytokines in the circulation associated with inflammation and EAE pathologies. In support of ongoing clinical trials using dietary strategies to treat MS patients, these findings support that a WFKD promotes a systemic anti-inflammatory milieu that mitigates autoimmune-induced demyelinating visual and motor deficits.

INTRODUCTION

Multiple sclerosis (MS), *neuromyelitis optica* (NMO), and a recently-classified family of "myelin oligodendrocyte glycoprotein (MOG)-antibody diseases" (MOG-ADs) [1] are autoimmune demyelinating diseases of the CNS that cause severe disabilities in patients. Motor, cognitive, and visual deficits from these diseases result in loss of mobility, balance and coordination, blindness, depression, fatigue, memory loss, and decreased quality of life. These diseases are more common in females, with onset typically occurring in the third and fourth decades of life (reviewed in [2-4]).

Despite numerous immune modulatory therapies approved for MS, these treatments are limited by efficacy, tolerability, expense, and adverse effects. For example, in a recent retrospective study of patients treated with Tecfidera, the most commonly prescribed oral medication for MS worldwide [5], 56% of patients discontinued the compound due to adverse effects (e.g., lymphopenia, gastrointestinal upset) or a perceived lack of efficacy [6], consistent with other reports [7,8]. In addition, currently-approved compounds and biologicals that target specific immune cells fail to spare the *homeostatic* populations and functions of the targeted cells. As a result, these interventions can compromise aspects of health independent of the autoimmune sequelae being targeted. For example, therapeutics that neutralize T_H17 effector T cells in autoimmune diseases typically do not discriminate between the pathogenic actions [9] and critical homeostatic functions of these cells in fighting fungal infections [10], restricting certain tumors from metastasizing [11], and in maintaining gut health and integrity [12-14].

The need for additional treatment strategies is further underscored by the increasing prevalence of patients testing positive for antinuclear antibodies (ANA), the most common biomarker of autoimmunity [15]. This increased incidence coincides with global increases in obesity, hyperglycemia, hyperinsulinemia, insulin resistance, dyslipidemia, and type 2 diabetes [16]. Mounting evidence points to the excessive consumption of ultra-processed foods containing highly-processed carbohydrates and pro-inflammatory fats as drivers of metabolic syndrome [17-19], poor health outcomes [20,21], and all-cause mortality [22]. These ultra-processed, hyperpalatable, calorically-dense foodstuffs promote hyperphagia [23], disrupt microbiome-host symbiosis, and result in systemic inflammation, all exacerbating factors of autoimmunity [24].

To overcome the shortcomings of current autoimmune treatments and reduce the toxic impacts of sugar-laden, processed foods, we are pursuing strategies that limit dietary carbohydrates but provide fiber. Our specific focus is the therapeutic application of ketogenic diets (KD). Nutritional ketosis has been used since the 1920s to treat children with drug-refractory seizures [25,26], and KDs have gained popularity for weight loss and as an anti-diabetic strategy because the diet suppresses hunger and reduces energy intake [27-29]. In fact, nutritional KDs, fasting, and exogenous ketone administration (i.e., induced ketosis) have shown therapeutic efficacy in disease models of MS, type 2 diabetes, Parkinson's disease, epilepsy, and Alzheimer's disease [30], inspiring small-scale clinical trials (reviewed in [31]). A recent trial involving a cohort of 262 diabetic and prediabetic individuals showed that at 2-year follow-up, patients consuming a KD had improvements in glycosylated hemoglobin (HbA1C), fasting glucose, fasting insulin, weight, blood pressure, triglycerides, alanine aminotransferase, and high-density lipoprotein, consistent with safety and tolerability for long-term adherence. Remarkably, 53% of enrolled patients achieved resolution of their type 2 diabetes [28]. These results are encouraging since insulin resistance and adiposity correlate with more severe disability scores for MS patients [32,33]. These and other findings (reviewed in [34,35]) have led to multiple clinical trials (e.g., NCT01538355, NCT03718247, NCT01915433, NCT05007483) including "Nutritional Approaches in Multiple Sclerosis" (NAMS; NCT03508414)), a randomized controlled clinical trial in Germany for patients with active MS to compare a KD versus a fasting protocol versus a fat-modified standard diet over an 18-month period [36].

KDs can differ in the composition of the individual diets but share at least two properties. The diets contain primarily fats with moderate protein content and low amounts of carbohydrates, typically in the range for humans of 0-70 g daily, excluding indigestible fiber. Secondly, KDs induce the liver to produce the ketone bodies β-hydroxybutyrate, acetoacetate, and acetone. People in nutritional ketosis have circulating ketones of 0.5 - 4mM with blood glucose less than 150mg/dL, irrespective of fasting or fed state. By contrast, pathological ketoacidosis associated with uncontrolled diabetes yields ketones exceeding 25mM and blood glucose greater than 240mg/dL.

The studies presented here were undertaken to determine whether a well-formulated KD (WFKD) preserves motor and visual function in both male and female mice during autoimmune challenge using the

mouse MOG-experimental autoimmune encephalomyelitis (MOG-EAE) model, hereafter referred to as 'EAE'. This model of autoimmune-mediated demyelination induces visual and motor pathologies similar to those experienced by patients with MS and NMO, and as such, has been instrumental in the development of multiple FDA-approved disease modifying therapies for MS [37]. The work here builds upon previous work with nutritional interventions using the EAE model. Caloric restriction has been shown to attenuate EAE motor deficits and to correlate with reduced levels of IL-6 and leptin [38]. Likewise, both a fast-mimicking diet [39-42] and a KD [40,43] reduce EAE motor disabilities. Additionally, a KD improves long-term potentiation, spatial learning, and memory in EAE mice [43].

The studies here are distinguished from and advance previous work in several ways. First, the present work compares female and male mice whereas previous ketogenic, calorie restriction, and fast-mimicking diet interventions were done only in females [38-42]. Second, previous studies focused on motor deficits and cognitive function but did not track ocular deficits. In this study, we longitudinally measured both motor function and vision. Ocular manifestations and vision loss are life-altering sequelae prevalent to MS and other autoimmune disorders (e.g., NMO, uveitis, Sjogren's syndrome) but are understudied compared to brain and spinal cord pathologies. 50% of MS patients experience optic nerve inflammation (aka. optic neuritis) during disease progression, and it is the presenting sign for ~20% of patients [44]. Optic neuritis flare-ups result in demyelination of the optic nerve and with successive episodes, retinal ganglion cells (RGCs) are damaged or killed leading to irreversible vision loss. We previously reported that EAE mice recapitulate the relapsing-remitting *monocular* vision loss experienced by MS patients [45]. Tracking both motor and visual function is also important to determine whether a given treatment shows anatomic-specific differences in efficacy, as we observed in EAE mice treated with dimethyl fumarate (DMF; Tecfidera) [6]. Third, the present study uses a WFKD enriched in medium chain triglycerides (MCTs; primarily caprylic acid (C8) and capric acid (C10)) along with flaxseed oil and canola oil as the sources of fat. This formulation was designed to minimize omega-6 (ω6) fatty acids and hydrogenated fats [46] and is distinguished from many KDs in the literature containing pro-inflammatory fats (e.g., corn oil, hydrogenated shortening, margarine) that impair metabolic health when consumed long-term [47]. In contrast to pro-inflammatory KDs that cause weight gain, this WFKD decreases body weight [46], and

importantly, is also distinguished from high fat chows containing pro-inflammatory fats and high sucrose/carbohydrate content used to induce obesity, metabolic syndrome, and type 2 diabetes in mice [48].

We report that a WFKD prevents both motor and visual deficits concomitant with preserving oligodendrocytes on the optic nerve in female and male mice undergoing EAE-induced autoimmunity. Fatty acid analyses of the plasma revealed that the WFKD increased circulating levels of multiple omega 3 (ω3) fatty acids associated with endogenous resolution pathways of acute inflammation. Analysis of cytokine and chemokine differences likewise showed that the WFKD reduced numerous factors associated with increased inflammation and MS pathogenicity. Together, these findings are consistent with a model in which the WFKD confers neuroprotection by promoting a systemic anti-inflammatory milieu.

RESULTS

A WFKD IS NON-OBESOGENIC AND INCREASES CIRCULATING KETONES.

Optic neuritis and visual disturbances are major sequelae of autoimmune demyelinating disease in humans [1,49,50]. To determine if a KD is efficacious in preserving both the motor and visual deficits induced by EAE and to address the sex-dependent effects of this dietary intervention, female and male mice were fed either a WFKD or an energetically-matched control diet (CD) for 2 weeks prior to MOG_{35-55} peptide immunization to enable acclimation to the diet based on previous strategies testing the impacts of C12, C16, and short chain fatty acids on CNS autoimmunity in the EAE model [51]. We maintained mice on their respective diets for the duration of the experiment during which motor scores, vision, and body weights were longitudinally tracked and blood was collected. 3 weeks post-immunization, mice were euthanized for post-mortem analyses (Fig. 1A). The WFKD contains medium chain triglycerides (MCTs), flaxseed oil, and canola oil as the sources of fat and is comprised of 77.1% fat, 22.4% protein, and 0.5% carbohydrates (Fig. 1B). A complete list of the diet ingredients is provided in Supplemental Fig. 1A. This diet was designed to minimize omega-6 (ω6) fatty acids and hydrogenated fats [46], and is distinguished from most KDs in the literature containing pro-inflammatory fats (e.g., corn oil, hydrogenated shortening, margarine) that impair metabolic health [47]. The WFKD used here is also distinguished from high fat chows containing pro-inflammatory fats *and* high sucrose/carbohydrate content used to induce obesity, metabolic syndrome, and type 2 diabetes in mice [48]. Mice consuming the WFKD had modest increases (< 5g) in weight during the acclimation period but weights decreased and were comparable to mice eating a CD within a week after immunization (Fig. 1C). As expected, the minimal carbohydrate content of the WFKD kept blood glucose levels relatively constant and increased non-fasting blood ketones in both sexes (Figs. 1D and 1E, respectively). Mice on the CD also had elevated circulating ketones 3 weeks after immunization likely due to motor deficits reducing their food intake (Fig. 1E).

A WFKD PREVENTS MOTOR AND VISUAL DEFICITS IN EAE MICE.

Remarkably, we observed that both female and male mice fed the WFKD were completely spared the ascending paralysis and motor deficits induced by the MOG-EAE model (Fig. 2A and 2B, respectively). We additionally measured visual acuity in mice by optokinetic tracking (OKT) at the initiation of the diets, prior to MOG_{35-55} immunization, and then daily beginning ~10 dpi, coincident with symptom onset (Fig. 1A). As we

reported previously [52], mice subjected to MOG-EAE typically undergo episodic *monocular* vision loss, mimicking what is experienced by patients with relapsing-remitting MS (RRMS) [53,54]. These deficits are readily detectable as diminished visual acuity by OKT [45,52]. The OKT measures each eye separately so all animals have a designated more affected (MA) and less affected (LA) eye. Consistent with the amelioration of motor deficits, the WFKD preserved vision in the MA and LA eyes of EAE females (Fig. 3A) and males (Fig. 3B). This preservation of visual function was accompanied by a sparing of Brn3A^{+} retinal ganglion cells (RGCs) (Figs. 3C-E). Specifically, the WFKD preserved RGCs in the central and medial retina when the data from females and males on each diet were combined (Fig. 3D). As we reported previously [52], RGCs in the peripheral retina are not typically lost during MOG-EAE (Figs. 3C and 3D). When RGC counts were analyzed as a function of both diet and sex, the preservation of RGCs by the WFKD was significant in the central retina for both females and males (Fig. 3E). Notably, RGC loss in longstanding MS cases is most prominent in the central retina [55].

A WFKD PRESERVES OLIGODENDROCYTES AND RESTRICTS INFLAMMATORY INFILTRATION OF THE OPTIC NERVE IN EAE MICE.

To complement the OKT and RGC analyses, immunohistochemistry (IHC) was performed on paraffin-embedded optic nerves (Fig. 4A). For each marker, labeling was quantified from sections captured along the entire length of the optic nerve, and optic nerves from non-EAE (i.e., healthy) mice were included for comparison. When considering diet and sex or diet independently of sex, the WFKD preserved CNPase labeling on the optic nerves, an oligodendrocyte marker and proxy of myelination (Figs. 4A and 4B). Specific CNPase labeling was quantified by comparing the staining encircling nuclei (Fig. 4A, arrowheads) with the remaining diffuse staining being non-specific background, as revealed by the optic nerves from healthy mice lacking this diffuse signal (Fig. 4A, top row, leftmost panel). Labeling for Iba1 and CD3 to mark macrophages/microglia and T cells, respectively, revealed that when combining the sexes, mice on the WFKD had reduced Iba1 and CD3 labeling of the optic nerve compared to mice on the CD (Figs. 4C and 4D, respectively, KD (F+M) versus CD (F+M)). Males on the WFKD had significantly decreased Iba1 and CD3 labeling compared to CD-fed males (Figs. 4A, 4C, and 4D, respectively). However, due to higher variability between samples for females on the WFKD, differences in Iba1 and CD3 labeling did not reach significance between the WFKD and CD groups (Figs. 4C and 4D, respectively). Notably, all groups had statistically

significant increases in Iba1 labeling compared to healthy (i.e., no-EAE) optic nerves (Figs. 4C). For CD3 labeling, females and males on the WFKD were comparable to no-EAE healthy mice whereas males and females on the CD showed significant increases (Fig. 4D). Principal components exploratory analysis confirmed that the relatively higher CNPase labeling and lower CD3 and Iba1 labeling observed in EAE mice on the WFKD correlated with lower motor and visual acuity deficits (Fig. 4E). The first principal component reveals that the WFKD-fed mice are statistically comparable to healthy mice but significantly different from the CD-fed group, presenting significantly improved motor and visual acuity scores, higher CNPase levels and lower CD3 and Iba1 levels. The second component suggests marginal separation of the healthy mice group (no EAE) from WFKD-fed mice, in terms of lower CD3 and Iba1 levels.

A WFKD INCREASES CIRCULATING ω3 FATTY ACIDS IN EAE MICE.

To gain mechanistic insights into the therapeutic efficacy of the WFKD, we analyzed a panel of circulating fatty acids in the plasma of EAE mice (Fig. 5A). Fatty acids that gave statistically significant changes are shown in the graphs (Fig. 5B-D) with the complete set of measurements presented in Supplemental Figs. 1C-E. Both females and males on the WFKD had elevated plasma levels of the ω3 fatty acids 18:3n3, 20:4n3, and 22:5n3 (Figs. 5B and 5C, respectively). Males also had elevated levels of the ω3 fatty acid 20:5n3 (Fig. 5C), the intermediate in the conversion of 20:4n3 to 22:5n3 [56]. 20:5n3 was also increased in WFKD-fed females but did not reach significance (Supplemental Fig. 1C). When the data from the sexes were combined, 18:3n3, 20:4n3, 20:5n3, and 22:5n3 were all elevated and the saturated fats, 14:0 and 16:0, were decreased in EAE mice fed the WFKD compared to their CD-fed counterparts (Fig. 5D). Likewise, the ratio of 20:4n6 to (20:5n3+22:6n3) (i.e., AA/(EPA+DHA)), a proxy of inflammatory status, was decreased in both sexes on the WFKD (Figs. 5B-5D). 20:5n3, 22:5n3, and 22:6n3 are biosynthetic precursors of E-series, T-series, and D-series resolvins, respectively. Resolvins are specialized pro-resolving lipid mediators (SPMs) that restrict the development of chronic inflammation by dampening acute inflammation (reviewed in [57]). We observed female-specific changes from the WFKD that included increased levels of 18:2n6, 20:1, and 22:1 along with decreases in 16:1, 18:1, 20:2n6, and 20:4n6 (Fig. 5B). EAE male mice on the WFKD had decreased circulating levels of 16:0 (Fig. 5C). We further found that 20:3n9 (eicosatrienoic acid; ETA) was decreased in the plasma of EAE females on the WFKD (Fig. 5B), approached significance in males (Supplemental Fig. 1D; p=0.054), and was

highly significant when the sexes were combined (Fig. 5D). 20:3n9 can be converted to the proinflammatory C3 and D3 leukotrienes [58] and elevated levels of this lipid in blood can be indicative of a state of essential fatty acid deficiency [59], although we did not detect other indicators of such a deficiency (e.g., 22:5n6) [60]. Together, these data are consistent with the WFKD conferring protection from EAE pathologies at least in part by enriching the systemic milieu with ω3 fatty acids associated with SPM-mediated neuroprotection and decreasing fatty acids, such as 20:3n9, that give rise to pro-inflammatory leukotrienes.

To determine which of the enriched circulating ω3 fatty acids in EAE mice consuming the WFKD were contributed directly by the diet, we analyzed the fatty acid content of the diets. Notably, compared to the CD, the WFKD was enriched 2.8-fold in 18:3n3 (α-linolenic acid; ALA) from the flaxseed oil in the diet (Supplemental Fig. 1B). 18:3n3 can be biosynthetically converted *in vivo* to the corresponding 20:4n3, 20:5n3, and 22:5n3 [56,61]. As 20:4n3, 20:5n3, and 22:5n3 were absent from the WFKD and CD diets (Supplemental Fig. 1B), we posit that such endogenous conversions account for the elevated levels of these ω3 fatty acids in the plasma of EAE mice consuming the WFKD (Fig. 5).

A WFKD REDUCES CIRCULATING PRO-INFLAMMATORY CYTOKINES IN EAE MICE.

Additional evidence supporting the anti-inflammatory milieu resulting from consumption of the WFKD came from a complementary analysis of 26 different cytokines and chemokines in the plasma 21dpi. Graphs are shown for factors that were statistically significantly changed as a function of diet (Fig. 6), with the complete set of cytokines analyzed shown in Supplemental Figs. 2A-C. For some factors, most or all samples were below the detection limit of the ELISA, precluding statistical comparisons (Supplemental Figs. 2A-D). In contrast to their counterparts eating the CD, male EAE mice eating the WFKD had decreased circulating levels of granulocyte-colony stimulating factor (G-CSF), C-X-C Motif Chemokine Ligand 2 (CXCL2), C-reactive protein (CRP), and C-C motif chemokine ligand 11 (CCL11) (Figs. 6A-D, respectively). Female EAE mice fed the WFKD also had decreased plasma levels of G-CSF and CXCL2 (Figs. 6A-B, respectively), along with lower interleukin-6 (IL-6) (Fig. 6E) and increased levels of monocyte-colony stimulating factor (M-CSF) (Fig. 6F). When males and females were combined, 4 circulating factors (G-CSF, CXCL2, CCL11, and IL-6) were significantly decreased in mice consuming the WFKD. CRP levels in WFKD female mice were in fact

comparable to the levels in WFKD male mice but curiously CRP was not elevated in female CD-fed mice undergoing EAE (Fig. 6C). Notably, G-CSF and CXCL2 were significantly reduced in both sexes on the WFKD.

EAE MICE FED A WFKD MOUNT A T-CELL RESPONSE TO MOG_{35-55} IMMUNIZATION.

To rule out that the protection conferred by the WFKD was not a consequence of the diet blunting an immune response to the MOG antigen, splenoctyes were isolated 21 dpi from EAE mice on each diet, stimulated *ex vivo* in culture with MOG_{35-55} peptide, and subsequently with PMA, iononmycin, and monensin prior to antibody labeling to identify activated T cells (i.e., $CD3^+$, $CD4^+$, $CD44^{++}$) and their respective intracellular levels of IL-17 and IFN-γ by flow cytometry (Supplemental Fig. 3). IL-17 and IFN-γ expression by MOG_{35-55} -activated splenic T cells is a signature EAE response to immunization with MOG (e.g., [62,63]). For comparison purposes, unstimulated sets of splenocytes from mice on either the WFKD or CD were similarly stained for intracellular IL-17 and IFN-γ. These analyses showed that the percent of live $CD3^+CD4^+$ $CD44^{++}$ T cells expressing IL-17 was comparable between diets whereas stimulated splenocytes from WFKD-fed animals had higher levels of IFN-γ expression than their CD-fed counterparts (Supplemental Figs. 3A and 3B). Notably, the level of activated $CD3^+CD4^+$ $CD44^{++}$ T cells was similar between the WFKD and CD groups (Supplemental Fig. 3C). We further observed a small of percentage of “breakthrough” mice consuming the WFKD that began to exhibit EAE symptoms ~ 21 dpi (Supplemental Fig. 3D). The mechanism driving this breakthrough is currently unknown. These lines of evidence support that although mice on the WFKD are protected from the overt pathologies induced by the EAE model, the underlying mechanism is not a failure to mount a T cell response to MOG antigen immunization. Collectively, the results presented demonstrate that the WFKD completely blocked the disease model in ≥90% of the mice and delayed disease onset by at least 10 days in the remaining 10%.

DISCUSSION

Previous work established that caloric restriction mitigates EAE disease severity [38]. In addition, both a fast-mimicking diet [39-42] and a KD [40,43] ameliorate EAE motor disabilities, and the KD improves long-term potentiation, spatial learning, and memory in EAE mice [43]. Our data corroborate that the KD spares motor functions (Fig. 2) and expand on this efficacy in multiple ways. We demonstrate that a WFKD preserves visual acuity (Fig. 3) and myelination of the optic nerve, with reduced infiltration of $CD3^+$ T cells and $Iba1^+$ phagocytes (Fig. 4). This protection correlates with the sparing of RGCs, the axons of which comprise the optic nerve (Fig. 3). We also show that the benefits of the WFKD extend comparably to male and female mice and that the WFKD increases circulating levels of the anti-inflammatory ω3 fatty acids 18:3n3, 20:4n3, 20:5n3, and 22:5n3 while decreasing the pro-inflammatory fatty acids 20:3n9 and 20:4n6 (Fig. 5D). Further, we detected WFKD-mediated differences in multiple circulating cytokines implicated in EAE and MS, with G-CSF and CXCL2 being reduced in both sexes (Fig. 6).

KDs have been used clinically since the 1920s to treat children with drug-refractory seizures [64-66], and have gained popularity as effective weight loss and anti-diabetes regimens [67,68]. As a result, many versions of this carbohydrate restriction regimen have emerged that differ in their respective fatty acid compositions. Since fats comprise > 70% of the calories in a typical KD, the specific fatty acids used to formulate these diets is of paramount importance with regards to cardiometabolic health and systemic inflammation. KDs can be enriched in ω6 fatty acids derived from vegetable oils, tofu, nuts, and seeds or in ω3 fatty acids derived from foods including fish, shellfish, and flaxseed. Although both ω6 and ω3 fats are essential for human health, excessive consumption of ω6 fatty acids coupled to insufficient consumption of ω3 fatty acids is linked to systemic inflammation, altered gut integrity, and metabolic syndrome characterized by obesity, hyperglycemia, hyperinsulinemia, insulin resistance, dyslipidemia, and type 2 diabetes [69-73]. It has been calculated that homo sapiens evolved consuming a 1:1 molar ratio of ω6:ω3 fatty acids but the Western diet consumed by many has an ω6:ω3 ratio of > 15:1 [70]. This imbalance has been attributed to the excessive consumption of hyperpalatable, ultra-processed foods laden with highly-processed carbohydrates and pro-inflammatory ω6 fats [24]. Coincident with reducing dietary ω6 fatty acids, compelling evidence favors that ω3 polyunsaturated fatty acids exert health benefits by reducing NLRP3 inflammasome activity [74], limiting the differentiation of pathogenic T cells (e.g., T_H17 cells) [75,76], and restricting neutrophil migration [77].

The WFKD used in the present study was designed to be non-obesogenic, anti-inflammatory, and to enrich ω3 fatty acids in the circulation [46]. In contrast, two previous EAE studies [40,43] used a KD containing corn oil and lard, fat sources that increase inflammation [78,79]. Although the KDs used in both studies were efficacious in mitigating the EAE sequelae analyzed, a consideration of the cardiometabolic health risks of chronically consuming high fat diets is of relevance to MS patients who likely will be utilizing these nutritional interventions over the long-term. Resistance to the use of fat-enriched diets as therapeutic strategies persists due to nutritional dogma among clinicians trained since the 1960s under the philosophy that dietary fats promote cardiovascular disease (e.g., [80]). This misconception has unfortunately been reinforced by reports that KDs consumed for several months by mice are pro-inflammatory and obesogenic (e.g., [47]). However, these adverse metabolic impacts come from feeding mice KD formulations enriched in pro-inflammatory hydrogenated shortening (i.e., *trans* fats) and corn oil (~60% ω6 18:2n6) (e.g., [47,81]). Although our studies lasted only 5 weeks, our observations support that the use of a WFKD enriched in ω3 fatty acids including the polyunsaturated fatty acid (PUFA), α-linolenic acid (ALA, 18:3n3), can elicit therapeutic benefits without promoting weight gain or increasing markers of inflammation.

Because different KD formulations mitigate EAE pathologies despite containing various pro- and anti-inflammatory fats [40,43], the therapeutic efficacy of KDs may derive from the production of ketones and/or the dramatic reduction in sugar and carbohydrate consumption common to these regimens. Consistent with these mechanisms, clinical work has shown that a KD was more efficacious in improving glycemic control and reducing the medications of obese diabetic patients as compared to a 55% carbohydrate low glycemic index diet [68]. In the context of autoimmune disease, mounting evidence implicates excess dietary carbohydrates in disease exacerbation. For example, high dietary glucose increases disease severity in the EAE model as well as a mouse model of colitis by promoting T_H17 cell differentiation via ROS-mediated TGF-β activation [82]. Human studies have shown that consumption of a KD by overweight individuals decreased weight, insulin resistance, and serum markers of inflammation (e.g., TNF-α, IL-6, IL-8, MCP-1) [83-85]. These normalizing effects on insulin sensitivity and insulin resistance benefit patients with metabolic syndrome and diabetes and likely extend to MS patients, as insulin resistance is associated with elevated MS disability scores [32,33]. Additionally, multiple pilot studies have shown promising responses in patients using (modified) paleo diets that eliminate or

dramatically reduce the consumption of simple carbohydrates, processed foods, and other putative disease aggravators (e.g., gluten, dairy, legumes) [86-93].

We speculate that an additional mechanistic contribution mediating the efficacy of the WFKD in the present study comes from the anti-inflammatory actions of resolvins, a family of SPMs derived from ALA. In alignment with this idea, elevated dietary consumption of 18:3n3 has been inversely linked with the risk of developing MS [94]. ALA was enriched in the WFKD diet compared to the CD (Supplemental Figs. 1B) and likewise in the plasma of EAE mice fed the WFKD compared to their CD counterparts (Figs. 5B-C). Moreover, the overall enrichment of ω3 fatty acids in the plasma of mice fed the WFKD may directly contribute to lower levels of inflammatory infiltrates in the more affected optic nerves (Fig. 4) as ω3 fatty acids reportedly decrease phagocytic infiltration to the corpus callosum following demyelinating injury and enhance lesion recovery [95].

The plasma of WFKD EAE females and males was enriched in ETA (20:4n3) and DPA (22:5n3) (Figs. 5B and 5C) and males were also enriched with EPA (20:5n3) (Fig. 5C). 20:5n3 and 22:5n3 are intermediate biosynthetic precursors of E-series and T-series resolvins, respectively. DHA (22:6n3) and arachidonic acid (20:4n6), the intermediates from which the Resolvin D-series and the lipoxins are synthesized, respectively, were not increased and arachidonic acid levels were reduced. However, the lack of elevated DHA and arachidonic acid does not necessarily preclude contributions from their respective SPMs as efficient synthesis reactions could limit the accumulation of these intermediates. A 2015 study by Poisson and colleagues using the MOG-EAE model and standard chow over a 45-day course showed PUFA metabolism is compromised during disease progression and that daily administration of exogenous Resolvin D1 decreased EAE pathologies [96]. Recent clinical work identified imbalances in pro-inflammatory eicosanoids and SPM levels in the plasma of MS patients as a function of disease progression and severity. In addition, these investigators discovered that the expression of multiple biosynthetic enzymes and receptors for SPMs were impaired in peripheral blood mononuclear cells from patients and that patient-derived monocytes were less responsive to SPMs in culture [97]. Based on these findings, it will be important moving forward to determine if increasing substrates for endogenous SPM synthesis using diets enriched in ALA (18:3n3), EPA (20:5n3), DHA (22:6n3), and/or other precursors is sufficient to restore SPM generation, signaling, and homeostasis in the EAE mouse model and ultimately, in MS patients (e.g., [98]). Thus, despite a lack of causal links, delineating the

immunomodulatory benefits and hazards of various dietary fatty acids in MS disease etiology and management is an emerging area of investigation (reviewed in [99]).

Fitting with the WFKD promoting a systemic anti-inflammatory milieu, we detected reductions in multiple pro-inflammatory cytokines and chemokines in male and female mice. G-CSF and CXCL2 were the two pro-inflammatory cytokines reduced in both sexes (Fig. 6A-B). G-CSF stimulates the production and maturation of granulocytes and neutrophils and its levels are typically kept low but rapidly increase in response to stress and inflammation. In the context of autoimmunity, G-CSF governs early signaling necessary for EAE disease induction [100] with the neutrophils produced by G-CSF driving multiple steps of EAE and MS progression (e.g., [101-105]), implying that reducing this factor in the circulation contributes to the efficacy of the WFKD to prevent EAE pathologies. Consistent with the benefits of limiting G-CSF levels, pilot studies showed that exogenous administration of this cytokine exacerbated relapse severity in some MS patients [106,107]. CXCL2 levels were also reduced by the WFKD in males and females (Fig. 6B). This factor is also known as macrophage inflammatory protein 2-α (MIP2-α), is produced by macrophages and neutrophils at sites of inflammation, and functions in recruiting neutrophils during inflammation [108]. Likewise, transient receptor potential melastatin 2 knockout mice have reduced CXCL2 and a suppression of neutrophil infiltration into the CNS during EAE [109]. Thus, reduced levels of circulating CXCL2 are consistent with disease mitigation and fit logically with the lower G-CSF levels observed that limit neutrophil maturation.

In conclusion, the work presented here demonstrates the efficacy of a WFKD to preserve both motor and visual function in female and male mice undergoing autoimmune demyelinating disease. Mechanistically, we propose that the WFKD exerts beneficial effects by limiting systemic inflammation and by reducing key cytokines involved in mediating the infiltration of T cells and phagocytic cells into the CNS. We further posit that this nutritional intervention provides an abundance of ω3 fatty acids for biosynthetic conversion into SPMs that in turn blunt acute inflammatory responses (to self-antigens) from transitioning to chronic inflammation and tissue damage. Future studies to test these hypotheses will include using the WFKD: (1) as an interventional strategy initiated coincident with symptom onset, (2) in additional models of autoimmune demyelinating disease, and (3) in comparison to other KD formulations to determine whether the fat composition of the diet governs efficacy or whether the therapeutic benefits derive primarily from circulating ketones, high fiber content, and/or from carbohydrate restriction and the ensuing reduction of insulin levels. As longer-term

nutritional intervention studies in patients are being pursued (e.g., [36]), complementary animal studies aim to facilitate the development and optimization of much-needed dietary interventions that are safe, efficacious, and sustainable for patients.

METHODS

Mice

Male and female C57BL/6J mice were housed in microisolator cages (n=4-5 per cage) under a 12-hr light/dark cycle. All animal care and experimental procedures were performed in compliance with ARRIVE guidelines, a Oklahoma Medical Research Foundation Institutional Animal Care and Use Committee (IACUC)-approved protocol, and complied with standards delineated by the Institute for Laboratory Animal Research. These studies adhered to The Association for Research in Vision and Ophthalmology (ARVO) statement for the Use of Animals in Research. All studies used C57BL/6J female and male mice. Breeders were purchased from Jackson Laboratories (stock # 000664). At the termination of experiments, mice were anesthetized before cardiac puncture to collect blood and subsequently sacrificed by CO_2 asphyxiation followed by cervical dislocation.

MOG-EAE

EAE was induced in 10-12 week old mice by subcutaneous flank injection of 150 µg of myelin oligodendrocyte glycoprotein peptide (residues 35-55; MOG35-55) (Genemed Synthesis, Inc., San Francisco, USA) emulsified in incomplete Freund's adjuvant (Thermo Fisher Scientific; DF0639606) supplemented with 5 mg/mL heat-inactivated *Mycobacterium tuberculosis* (Thermo Fisher Scientific; DF3114338). Mice were injected intraperitoneally with 250 ng *Bordetella pertussis* toxin (List Biological Laboratories, Inc. #181) the day of, and 2 days following, MOG_{35-55} immunization. 21-23 days post-immunization, mice were euthanized for post-mortem histology. Manifestations of progressive ascending paralysis of classical EAE were assessed daily, as previously described [6,45,52], using a standard scoring system: 0 – no disease, 0.5 – reduced tail tone, 1- loss of tail tone, 1.5 – limp tail and ataxia, 2- hind limb paresis, 2.5 – one hind limb paralyzed, 3- complete hind limb paralysis, 3.5 – complete hind limb paralysis and forelimb weakness, 4- hind limb paralysis and forelimb paresis, 5- moribund or dead. Mice were weighed daily to ensure weight loss did not exceed 25% of starting weight at the time of immunization.

Visual acuity assessment

Visual acuity threshold was measured daily by OKT response using Optometry software and apparatus (Cerebral Mechanics Inc., Alberta, Canada) as previously described [6,45,52]. Briefly, mice are surrounded by a

virtual cylinder consisting of vertical lines projected on 4 computer screens comprising a box surrounding the animal. The vertical lines rotate at varying frequencies, and tracking behavior is assessed in a stepwise manner as the thickness of the lines are reduced. Visual acuity is represented as the highest spatial frequency at which mice track the rotating cylinder. Optokinetic tracking is a temporal-to-nasal reflex, and therefore counter-clockwise and clockwise rotations exclusively test the right and left eye, respectively. When EAE-induced motor deficits rendered mice without the balance and stability to adequately perform OKT testing, a measurement was not recorded for the affected mouse on that day.

Retinal flatmount analysis

Retinal flatmounts were prepared and RGCs labeled and quantified as described [6,45,52] using anti-Brn3a (goat; Santa Cruz, Santa Cruz, CA; sc31984; 1:500), $Alexa_{546nm}$ Fluor-conjugated donkey anti-goat IgG (Molecular Probes; 1:1,000), and Hoechst 33342 (2 µg/mL) all diluted in 3% BSA/10% donkey serum/PBS. Retinas were washed in PBS before mounting with Prolong Gold mounting medium (Life Technologies, Grand Island, NY) and examined with a Nikon 80i microscope with a 60X objective. Images were captured with a DXM1200C camera using NIS-Elements software (Nikon, Inc. Tokyo, Japan). Photomicrographs were captured from the four leaflets comprising the flatmount with representative images captured from the peripheral, medial, and central retina within each quadrant, yielding 12 pictures per retina. Images were cropped to 325 μm^2 and contrast-enhanced in Adobe Photoshop 8.0. Brn3a-positive RGCs were counted manually.

Diet compositions

Teklad control (TD.170645) and ketogenic (TD.10911) diets were obtained from Envigo, Inc., and custom formulated with the assistance of a company nutritionist based on [46]. At the macronutrient level, the ketogenic diet provides 4.7 Kcal/g with 22.4% Kcal from protein, 0.5% Kcal from carbohydrate, and 77.1% Kcal from fat. The control diet provides 3.6 Kcal/g with 20.4% Kcal from protein, 69.3% Kcal from carbohydrate, and 10.4% Kcal from fat. Diet ingredients are provided in Fig. 1B and in Supplemental Fig. 1. Diet and hydration were provided ad libitum.

Fatty acid analysis

Plasma fatty acid profiles were determined by extracting total lipids from 40-50 µl of plasma following the method of Bligh and Dyer [110] with slight modifications [111]. The purified total lipid extracts were stored under nitrogen until use. To these lipid extracts, 50 nmol each of 15:0 and 17:0 internal standards were added and the total extracts subjected to acid hydrolysis/methanolysis to generate fatty acid methyl esters (FAMEs) [112]. All reagents for fatty acid extraction and derivatization were of the highest quality available from Sigma-Aldrich. FAMEs were identified using an Agilent Technologies 7890A gas chromatograph with a 5975C inert XL mass spectrometer detector (Agilent Technologies, Lexington, MA) as described [112]. The gas chromatograph-mass spectrometer was operated in the electron impact total ion monitoring mode. The injection volume was 1 µl and the inlet, held at 325°C, was set to pulsed splitless mode. An Agilent Technologies HP-5MS column (30 m × 0.25 mm × 0.25 µm) was used with a helium carrier gas flow rate of 1.2 ml/min. The oven temperature began at 130°C for 1.0 min, was ramped to 170°C at 6.8°C/min, and was then ramped to 215°C at 2.9°C/min. After holding at 215°C for 15.0 min, the oven was ramped to 260°C at 20°C/min and held for 5.0 min. The oven was then ramped to 325°C at 15°C/min and held for 18.0 min. The mass spectrometer transfer line, ion source, and quadrupole temperatures were 325°C, 230°C, and 150°C, respectively.

FAMEs were quantified using an Agilent Technologies 6890N gas chromatograph with flame ionization detector (GC-FID) [113]. Sample concentrations were determined by comparison to internal standards 15:0 and 17:0. The injection volume was 1 µl and the inlet, held at 290°C, was set to pulsed split mode (10:1 ratio). An Agilent Technologies DB-23 column (60 m × 0.32 mm × 0.25 µm) was used with a hydrogen carrier gas constant pressure of 13.1 psi. The oven temperature began at 130°C for 0.8 min, was ramped to 170°C at 8.2°C/min, and was then ramped to 215°C at 3.5°C/min. After holding at 215°C for 9.5 min, the oven was ramped to 230°C at 50°C/min, and was then held for 8 min. The oven was then ramped to 290°C at 12.0°C/min and was held for 12 min. The detector was held at 290°C. Data for the diets is represented as µg of each fatty acid per mg of diet, and data from plasma is represented as nmol of fatty acid per mg of protein.

Ex vivo stimulation of splenocytes

21 days post-immunization, single cell suspensions from spleens were prepared. 2 x 10^6 cells were plated in triplicate in complete RPMI (supplemented with 10% FBS, 2mM L-glutamine, 1% pen/strep, 2mM β-mercaptoethanol, non-essential amino acids, 1mM sodium pyruvate). 10µg/mL MOG was added to the "stimulated" wells and incubated at 37℃ for 24 hrs. For the final 5 hrs of the 24-hr incubation, samples were spiked with 50ng/mL PMA (Sigma, Inc. cat # P1585), 500ng/mL ionomycin (Sigma, Inc. cat # IO634), and BD Golgi StopTM containing monensin (0.66µL/mL; BD Biosciences). Cells from triplicate wells were combined, stained with a fixable viability dye (Biolegend) and treated with Fc block (TruStain FcX PLUS; BioLegend, Inc. cat # 156604) subsequent to staining with the following anti-mouse Abs against cell surface markers (all Abs from eBioscience, Inc.): anti-CD3 (145-2C11), anti-CD4 (GK1.5), anti-CD8 (53-6.7), and anti-CD44 (IM7). Cells were fixed and permeabilized with BD Cytofix/CytopermTM Plus (BD Biosciences, Inc.) and stained with anti-IL17 (TC11-18H10.1) and anti-IFN-γ (XMG1.2) to detect the respective cytokines intracellularly. Samples were processed on a LSRII flow cytometer (BD Biosciences) and data analyzed with FlowJoTM version 10.7.1 software (BD Biosciences, Inc.).

Blood and ketone measurements

Blood ketone levels (non-fasting) were measured with a Precision Xtra Blood Ketone Monitoring System and fasting blood sugar was measured after 6 hrs of food withdrawal using a True Metrix Blood Glucose Meter. Blood was drawn from the tail vein.

Cytokine analyses

The levels of 26 cytokines and chemokines in the plasma of EAE mice 21 days post-immunization (dpi) were quantified using custom xMAP multiplex cytokine panels from Biotechne, Inc. according to the manufacturer's recommendations and processed in the OMRF Arthritis and Clinical Immunology Human Phenotyping Core.

Immunohistochemistry of optic nerves

To assess oligodendrocytes (as a marker of de/myelination) as well as lymphocyte and macrophage infiltration, we incubated sequential de-paraffinized sections with anti- 2',3'-cyclic-nucleotide 3'-phosphodiesterase (CNPase) (mouse CNPase: 1:200 dilution; Biolegend, Inc.), anti-CD3 (rabbit; 1:250; Abcam) or anti-Iba1

(mouse; 1:200; Millipore, Inc.) antibodies after antigen retrieval in R-buffer B. Images were captured using a Nikon fluorescent microscope. Quantification of staining was performed using FIJI Software. CNPase, Iba1, and CD3 staining on sections spanning the entire length of the optic nerve were quantified by a masked experimentalist using representative images from both ends and the middle of the optic nerve. The number of positive cells within a defined area were counted using the Cell Counter Plugin, and the number of positive-stained cells per 10,000 pixels was calculated and averaged for each optic nerve.

Statistical analysis

Confidence intervals and p values for the statistical significance of each studied effect in the longitudinal or binocular data were determined by fitting the data to a linear mixed-effects model, using the lme function implemented in the nlme R package, as detailed in [45,114-116]. This function is an extended version of regular linear regression but can accommodate complex data collection design features, such as longitudinal measurements, nested layers, and within-group correlation. Standard testing methods, such as the Student's unpaired t-test and the Mann–Whitney exact test, with Bonferroni correction for multiple testing, were employed when no embedding was involved. Graphpad Prism 9 was used to display the results. Percentages in Supplemental Figure 2 were compared with Fisher test. Pairwise testing for differences in marker levels among the five mice groups in Figure 4 was performed following log transformations for improving normality by unequal group variance ANOVA and Tukey's post hoc multiple comparisons test adjustment. Principal component exploratory analysis (PCA) and biplot generation were carried out with specific functions from stats package in R. Multidimensional 95% confidence regions were added to the biplot using the draw.ellipse function from the plotrix package.

REFERENCES

1 Reindl, M. & Rostasy, K. MOG antibody-associated diseases. *Neurology(R) neuroimmunology & neuroinflammation* **2**, e60, doi:10.1212/NXI.0000000000000060 (2015).

2 Leray, E., Moreau, T., Fromont, A. & Edan, G. Epidemiology of multiple sclerosis. *Rev Neurol (Paris)* **172**, 3-13, doi:10.1016/j.neurol.2015.10.006 (2016).

3 Tullman, M. J. Overview of the epidemiology, diagnosis, and disease progression associated with multiple sclerosis. *Am J Manag Care* **19**, S15-20 (2013).

4 Walton, C. *et al.* Rising prevalence of multiple sclerosis worldwide: Insights from the Atlas of MS, third edition. *Multiple sclerosis* **26**, 1816-1821, doi:10.1177/1352458520970841 (2020).

5 Mills, E. A., Ogrodnik, M. A., Plave, A. & Mao-Draayer, Y. Emerging Understanding of the Mechanism of Action for Dimethyl Fumarate in the Treatment of Multiple Sclerosis. *Frontiers in neurology* **9**, 5, doi:10.3389/fneur.2018.00005 (2018).

6 Zyla, K. *et al.* Dimethyl fumarate mitigates optic neuritis. *Mol Vis* **25**, 446-461 (2019).

7 Hersh, C. M. *et al.* Comparative efficacy and discontinuation of dimethyl fumarate and fingolimod in clinical practice at 24-month follow-up. *Mult Scler J Exp Transl Clin* **3**, 2055217317715485, doi:10.1177/2055217317715485 (2017).

8 Vollmer, B. *et al.* Discontinuation and comparative effectiveness of dimethyl fumarate and fingolimod in 2 centers. *Neurol Clin Pract* **8**, 292-301, doi:10.1212/CPJ.0000000000000487 (2018).

9 Zhao, Y., Liu, Z., Qin, L., Wang, T. & Bai, O. Insights into the mechanisms of Th17 differentiation and the Yin-Yang of Th17 cells in human diseases. *Mol Immunol* **134**, 109-117, doi:10.1016/j.molimm.2021.03.010 (2021).

10 Dutzan, N. *et al.* A dysbiotic microbiome triggers TH17 cells to mediate oral mucosal immunopathology in mice and humans. *Science translational medicine* **10**, doi:10.1126/scitranslmed.aat0797 (2018).

11 You, R. *et al.* IL17A Regulates Tumor Latency and Metastasis in Lung Adeno and Squamous SQ.2b and AD.1 Cancer. *Cancer Immunol Res* **6**, 645-657, doi:10.1158/2326-6066.CIR-17-0554 (2018).

12 Lee, J. Y. *et al.* Serum Amyloid A Proteins Induce Pathogenic Th17 Cells and Promote Inflammatory Disease. *Cell* **183**, 2036-2039, doi:10.1016/j.cell.2020.12.008 (2020).

13 Sano, T. *et al.* An IL-23R/IL-22 Circuit Regulates Epithelial Serum Amyloid A to Promote Local Effector Th17 Responses. *Cell* **163**, 381-393, doi:10.1016/j.cell.2015.08.061 (2015).

14 Yang, K. & Chi, H. Metabolic Control of Th17 Cell Generation and CNS Inflammation. *J Neurol Neurophysiol* **Suppl 12**, doi:10.4172/2155-9562.S12-004 (2014).

15 Dinse, G. E. *et al.* Increasing Prevalence of Antinuclear Antibodies in the United States. *Arthritis Rheumatol* **72**, 1026-1035, doi:10.1002/art.41214 (2020).

16 Versini, M., Jeandel, P. Y., Rosenthal, E. & Shoenfeld, Y. Obesity in autoimmune diseases: not a passive bystander. *Autoimmun Rev* **13**, 981-1000, doi:10.1016/j.autrev.2014.07.001 (2014).

17 Ivancovsky-Wajcman, D. *et al.* Ultra-processed food is associated with features of metabolic syndrome and non-alcoholic fatty liver disease. *Liver Int* **41**, 2635-2645, doi:10.1111/liv.14996 (2021).

18 Martinez Steele, E., Juul, F., Neri, D., Rauber, F. & Monteiro, C. A. Dietary share of ultra-processed foods and metabolic syndrome in the US adult population. *Prev Med* **125**, 40-48, doi:10.1016/j.ypmed.2019.05.004 (2019).

19 Tavares, L. F., Fonseca, S. C., Garcia Rosa, M. L. & Yokoo, E. M. Relationship between ultra-processed foods and metabolic syndrome in adolescents from a Brazilian Family Doctor Program. *Public Health Nutr* **15**, 82-87, doi:10.1017/S1368980011001571 (2012).

20 Fiolet, T. *et al.* Consumption of ultra-processed foods and cancer risk: results from NutriNet-Sante prospective cohort. *BMJ* **360**, k322, doi:10.1136/bmj.k322 (2018).

21 Mendonca, R. D. *et al.* Ultra-Processed Food Consumption and the Incidence of Hypertension in a Mediterranean Cohort: The Seguimiento Universidad de Navarra Project. *Am J Hypertens* **30**, 358-366, doi:10.1093/ajh/hpw137 (2017).

22 Schnabel, L. *et al.* Association Between Ultraprocessed Food Consumption and Risk of Mortality Among Middle-aged Adults in France. *JAMA Intern Med* **179**, 490-498, doi:10.1001/jamainternmed.2018.7289 (2019).

23 Hall, K. D. *et al.* Ultra-Processed Diets Cause Excess Calorie Intake and Weight Gain: An Inpatient Randomized Controlled Trial of Ad Libitum Food Intake. *Cell metabolism* **30**, 67-77 e63, doi:10.1016/j.cmet.2019.05.008 (2019).

24 Thorburn, A. N., Macia, L. & Mackay, C. R. Diet, metabolites, and "western-lifestyle" inflammatory diseases. *Immunity* **40**, 833-842, doi:10.1016/j.immuni.2014.05.014 (2014).
25 Martin-McGill, K. J., Jackson, C. F., Bresnahan, R., Levy, R. G. & Cooper, P. N. Ketogenic diets for drug-resistant epilepsy. *Cochrane Database Syst Rev* **11**, CD001903, doi:10.1002/14651858.CD001903.pub4 (2018).
26 Wheless, J. W. History of the ketogenic diet. *Epilepsia* **49 Suppl 8**, 3-5, doi:10.1111/j.1528-1167.2008.01821.x (2008).
27 Abbasi, J. Interest in the Ketogenic Diet Grows for Weight Loss and Type 2 Diabetes. *JAMA* **319**, 215-217, doi:10.1001/jama.2017.20639 (2018).
28 Athinarayanan, S. J. *et al.* Long-Term Effects of a Novel Continuous Remote Care Intervention Including Nutritional Ketosis for the Management of Type 2 Diabetes: A 2-Year Non-randomized Clinical Trial. *Front Endocrinol (Lausanne)* **10**, 348, doi:10.3389/fendo.2019.00348 (2019).
29 Saslow, L. R. *et al.* Twelve-month outcomes of a randomized trial of a moderate-carbohydrate versus very low-carbohydrate diet in overweight adults with type 2 diabetes mellitus or prediabetes. *Nutr Diabetes* **7**, 304, doi:10.1038/s41387-017-0006-9 (2017).
30 McDonald, T. J. W. & Cervenka, M. C. Lessons learned from recent clinical trials of ketogenic diet therapies in adults. *Curr Opin Clin Nutr Metab Care* **22**, 418-424, doi:10.1097/MCO.0000000000000596 (2019).
31 Dewsbury, L. S., Lim, C. K. & Steiner, G. Z. The Efficacy of Ketogenic Therapies in the Clinical Management of People with Neurodegenerative Disease: A Systematic Review. *Adv Nutr* **12**, 1571-1593, doi:10.1093/advances/nmaa180 (2021).
32 Oliveira, S. R. *et al.* Insulin resistance, atherogenicity, and iron metabolism in multiple sclerosis with and without depression: Associations with inflammatory and oxidative stress biomarkers and uric acid. *Psychiatry Res* **250**, 113-120, doi:10.1016/j.psychres.2016.12.039 (2017).
33 Oliveira, S. R. *et al.* Disability in patients with multiple sclerosis: influence of insulin resistance, adiposity, and oxidative stress. *Nutrition* **30**, 268-273, doi:10.1016/j.nut.2013.08.001 (2014).
34 Storoni, M. & Plant, G. T. The Therapeutic Potential of the Ketogenic Diet in Treating Progressive Multiple Sclerosis. *Mult Scler Int* **2015**, 681289, doi:10.1155/2015/681289 (2015).
35 Wilhelm, C., Surendar, J. & Karagiannis, F. Enemy or ally? Fasting as an essential regulator of immune responses. *Trends in immunology* **42**, 389-400, doi:10.1016/j.it.2021.03.007 (2021).
36 Bahr, L. S. *et al.* Ketogenic diet and fasting diet as Nutritional Approaches in Multiple Sclerosis (NAMS): protocol of a randomized controlled study. *Trials* **21**, 3, doi:10.1186/s13063-019-3928-9 (2020).
37 Glatigny, S. & Bettelli, E. Experimental Autoimmune Encephalomyelitis (EAE) as Animal Models of Multiple Sclerosis (MS). *Cold Spring Harb Perspect Med* **8**, doi:10.1101/cshperspect.a028977 (2018).
38 Piccio, L., Stark, J. L. & Cross, A. H. Chronic calorie restriction attenuates experimental autoimmune encephalomyelitis. *J Leukoc Biol* **84**, 940-948, doi:10.1189/jlb.0208133 (2008).
39 Bai, M. *et al.* Intermittent caloric restriction with a modified fasting-mimicking diet ameliorates autoimmunity and promotes recovery in a mouse model of multiple sclerosis. *J Nutr Biochem* **87**, 108493, doi:10.1016/j.jnutbio.2020.108493 (2021).
40 Choi, I. Y. *et al.* A Diet Mimicking Fasting Promotes Regeneration and Reduces Autoimmunity and Multiple Sclerosis Symptoms. *Cell Rep* **15**, 2136-2146, doi:10.1016/j.celrep.2016.05.009 (2016).
41 Kafami, L. *et al.* Intermittent feeding attenuates clinical course of experimental autoimmune encephalomyelitis in C57BL/6 mice. *Avicenna J Med Biotechnol* **2**, 47-52 (2010).
42 Razeghi Jahromi, S. *et al.* Effects of Intermittent Fasting on Experimental Autoimune Encephalomyelitis in C57BL/6 Mice. *Iran J Allergy Asthma Immunol* **15**, 212-219 (2016).
43 Kim, D. Y. *et al.* Inflammation-mediated memory dysfunction and effects of a ketogenic diet in a murine model of multiple sclerosis. *PLoS One* **7**, e35476, doi:10.1371/journal.pone.0035476 (2012).
44 Wilhelm, H. & Schabet, M. The Diagnosis and Treatment of Optic Neuritis. *Dtsch Arztebl Int* **112**, 616-625; quiz 626, doi:10.3238/arztebl.2015.0616 (2015).
45 Larabee, C. M. *et al.* Loss of Nrf2 exacerbates the visual deficits and optic neuritis elicited by experimental autoimmune encephalomyelitis. *Mol Vis* **22**, 1503-1513 (2016).
46 Brownlow, M. L., Benner, L., D'Agostino, D., Gordon, M. N. & Morgan, D. Ketogenic diet improves motor performance but not cognition in two mouse models of Alzheimer's pathology. *PLoS One* **8**, e75713, doi:10.1371/journal.pone.0075713 (2013).
47 Goldberg, E. L. *et al.* Ketogenesis activates metabolically protective gammadelta T cells in visceral adipose tissue. *Nat Metab* **2**, 50-61, doi:10.1038/s42255-019-0160-6 (2020).

48 Virgen-Carrillo, C. A., de Los Rios, D. L. H., Torres, K. R. & Moreno, A. G. M. Diagnostic criteria for metabolic syndrome in diet-induced rodent models: A systematic review. *Curr Diabetes Rev*, doi:10.2174/1573399817666210414103730 (2021).
49 Kale, N. Optic neuritis as an early sign of multiple sclerosis. *Eye Brain* **8**, 195-202, doi:10.2147/EB.S54131 (2016).
50 Papp, V. *et al.* Worldwide Incidence and Prevalence of Neuromyelitis Optica: A Systematic Review. *Neurology* **96**, 59-77, doi:10.1212/WNL.0000000000011153 (2021).
51 Haghikia, A. *et al.* Dietary Fatty Acids Directly Impact Central Nervous System Autoimmunity via the Small Intestine. *Immunity* **43**, 817-829, doi:10.1016/j.immuni.2015.09.007 (2015).
52 Larabee, C. M. *et al.* Myelin-specific Th17 cells induce severe relapsing optic neuritis with irreversible loss of retinal ganglion cells in C57BL/6 mice. *Mol Vis* **22**, 332-341 (2016).
53 The clinical profile of optic neuritis. Experience of the Optic Neuritis Treatment Trial. Optic Neuritis Study Group. *Arch Ophthalmol* **109**, 1673-1678 (1991).
54 Atkins, E. J., Biousse, V. & Newman, N. J. The natural history of optic neuritis. *Rev Neurol Dis* **3**, 45-56 (2006).
55 Green, A. J., McQuaid, S., Hauser, S. L., Allen, I. V. & Lyness, R. Ocular pathology in multiple sclerosis: retinal atrophy and inflammation irrespective of disease duration. *Brain* **133**, 1591-1601, doi:10.1093/brain/awq080 (2010).
56 Hulbert, A. J., Kelly, M. A. & Abbott, S. K. Polyunsaturated fats, membrane lipids and animal longevity. *J Comp Physiol B* **184**, 149-166, doi:10.1007/s00360-013-0786-8 (2014).
57 Zahoor, I. & Giri, S. Specialized Pro-Resolving Lipid Mediators: Emerging Therapeutic Candidates for Multiple Sclerosis. *Clinical reviews in allergy & immunology* **60**, 147-163, doi:10.1007/s12016-020-08796-4 (2021).
58 Hammarstrom, S. Conversion of 5,8,11-eicosatrienoic acid to leukotrienes C3 and D3. *J Biol Chem* **256**, 2275-2279 (1981).
59 Ichi, I. *et al.* Identification of genes and pathways involved in the synthesis of Mead acid (20:3n-9), an indicator of essential fatty acid deficiency. *Biochim Biophys Acta* **1841**, 204-213, doi:10.1016/j.bbalip.2013.10.013 (2014).
60 Bourre, J. M. *et al.* Function of dietary polyunsaturated fatty acids in the nervous system. *Prostaglandins Leukot Essent Fatty Acids* **48**, 5-15, doi:10.1016/0952-3278(93)90003-f (1993).
61 Burdge, G. C. & Wootton, S. A. Conversion of alpha-linolenic acid to eicosapentaenoic, docosapentaenoic and docosahexaenoic acids in young women. *Br J Nutr* **88**, 411-420, doi:10.1079/BJN2002689 (2002).
62 El-behi, M., Rostami, A. & Ciric, B. Current views on the roles of Th1 and Th17 cells in experimental autoimmune encephalomyelitis. *J Neuroimmune Pharmacol* **5**, 189-197, doi:10.1007/s11481-009-9188-9 (2010).
63 Imler, T. J., Jr. & Petro, T. M. Decreased severity of experimental autoimmune encephalomyelitis during resveratrol administration is associated with increased IL-17+IL-10+ T cells, CD4(-) IFN-gamma+ cells, and decreased macrophage IL-6 expression. *Int Immunopharmacol* **9**, 134-143, doi:10.1016/j.intimp.2008.10.015 (2009).
64 D'Andrea Meira, I. *et al.* Ketogenic Diet and Epilepsy: What We Know So Far. *Front Neurosci* **13**, 5, doi:10.3389/fnins.2019.00005 (2019).
65 Freeman, J. M. *et al.* The efficacy of the ketogenic diet-1998: a prospective evaluation of intervention in 150 children. *Pediatrics* **102**, 1358-1363, doi:10.1542/peds.102.6.1358 (1998).
66 Lefevre, F. & Aronson, N. Ketogenic diet for the treatment of refractory epilepsy in children: A systematic review of efficacy. *Pediatrics* **105**, E46, doi:10.1542/peds.105.4.e46 (2000).
67 Dashti, H. M. *et al.* Beneficial effects of ketogenic diet in obese diabetic subjects. *Mol Cell Biochem* **302**, 249-256, doi:10.1007/s11010-007-9448-z (2007).
68 Westman, E. C., Yancy, W. S., Jr., Mavropoulos, J. C., Marquart, M. & McDuffie, J. R. The effect of a low-carbohydrate, ketogenic diet versus a low-glycemic index diet on glycemic control in type 2 diabetes mellitus. *Nutr Metab (Lond)* **5**, 36, doi:10.1186/1743-7075-5-36 (2008).
69 Cordain, L. *et al.* Origins and evolution of the Western diet: health implications for the 21st century. *Am J Clin Nutr* **81**, 341-354, doi:10.1093/ajcn.81.2.341 (2005).
70 Simopoulos, A. P. The importance of the ratio of omega-6/omega-3 essential fatty acids. *Biomed Pharmacother* **56**, 365-379, doi:10.1016/s0753-3322(02)00253-6 (2002).

71 Simopoulos, A. P. Omega-3 fatty acids in inflammation and autoimmune diseases. *J Am Coll Nutr* **21**, 495-505, doi:10.1080/07315724.2002.10719248 (2002).
72 Simopoulos, A. P. An Increase in the Omega-6/Omega-3 Fatty Acid Ratio Increases the Risk for Obesity. *Nutrients* **8**, 128, doi:10.3390/nu8030128 (2016).
73 Simopoulos, A. P. & DiNicolantonio, J. J. The importance of a balanced omega-6 to omega-3 ratio in the prevention and management of obesity. *Open Heart* **3**, e000385, doi:10.1136/openhrt-2015-000385 (2016).
74 Yan, Y. *et al.* Omega-3 fatty acids prevent inflammation and metabolic disorder through inhibition of NLRP3 inflammasome activation. *Immunity* **38**, 1154-1163, doi:10.1016/j.immuni.2013.05.015 (2013).
75 Allen, M. J. *et al.* n-3 PUFAs reduce T-helper 17 cell differentiation by decreasing responsiveness to interleukin-6 in isolated mouse splenic CD4(+) T cells. *J Nutr* **144**, 1306-1313, doi:10.3945/jn.114.194407 (2014).
76 Monk, J. M., Hou, T. Y., Turk, H. F., McMurray, D. N. & Chapkin, R. S. n3 PUFAs reduce mouse CD4+ T-cell ex vivo polarization into Th17 cells. *J Nutr* **143**, 1501-1508, doi:10.3945/jn.113.178178 (2013).
77 Ferrante, A. *et al.* Neutrophil migration inhibitory properties of polyunsaturated fatty acids. The role of fatty acid structure, metabolism, and possible second messenger systems. *J Clin Invest* **93**, 1063-1070, doi:10.1172/JCI117056 (1994).
78 Garbow, J. R. *et al.* Hepatic steatosis, inflammation, and ER stress in mice maintained long term on a very low-carbohydrate ketogenic diet. *Am J Physiol Gastrointest Liver Physiol* **300**, G956-967, doi:10.1152/ajpgi.00539.2010 (2011).
79 Jornayvaz, F. R. *et al.* A high-fat, ketogenic diet causes hepatic insulin resistance in mice, despite increasing energy expenditure and preventing weight gain. *Am J Physiol Endocrinol Metab* **299**, E808-815, doi:10.1152/ajpendo.00361.2010 (2010).
80 La Berge, A. F. How the ideology of low fat conquered america. *J Hist Med Allied Sci* **63**, 139-177, doi:10.1093/jhmas/jrn001 (2008).
81 Li, Y. *et al.* Ketogenic Diets Induced Glucose Intolerance and Lipid Accumulation in Mice with Alterations in Gut Microbiota and Metabolites. *mBio* **12**, doi:10.1128/mBio.03601-20 (2021).
82 Zhang, D. *et al.* High Glucose Intake Exacerbates Autoimmunity through Reactive-Oxygen-Species-Mediated TGF-beta Cytokine Activation. *Immunity*, doi:10.1016/j.immuni.2019.08.001 (2019).
83 Forsythe, C. E. *et al.* Comparison of low fat and low carbohydrate diets on circulating fatty acid composition and markers of inflammation. *Lipids* **43**, 65-77, doi:10.1007/s11745-007-3132-7 (2008).
84 Hallberg, S. J. *et al.* Effectiveness and Safety of a Novel Care Model for the Management of Type 2 Diabetes at 1 Year: An Open-Label, Non-Randomized, Controlled Study. *Diabetes Ther* **9**, 583-612, doi:10.1007/s13300-018-0373-9 (2018).
85 Hyde, P. N. *et al.* Dietary carbohydrate restriction improves metabolic syndrome independent of weight loss. *JCI Insight* **4**, doi:10.1172/jci.insight.128308 (2019).
86 Bisht, B. *et al.* A multimodal intervention for patients with secondary progressive multiple sclerosis: feasibility and effect on fatigue. *J Altern Complement Med* **20**, 347-355, doi:10.1089/acm.2013.0188 (2014).
87 Bisht, B. *et al.* Multimodal intervention improves fatigue and quality of life in subjects with progressive multiple sclerosis: a pilot study. *Degener Neurol Neuromuscul Dis* **5**, 19-35, doi:10.2147/DNND.S76523 (2015).
88 Bisht, B. *et al.* Effects of a multimodal intervention on gait and balance of subjects with progressive multiple sclerosis: a prospective longitudinal pilot study. *Degener Neurol Neuromuscul Dis* **7**, 79-93, doi:10.2147/DNND.S128872 (2017).
89 Fellows Maxwell, K. *et al.* Lipid profile is associated with decreased fatigue in individuals with progressive multiple sclerosis following a diet-based intervention: Results from a pilot study. *PLoS One* **14**, e0218075, doi:10.1371/journal.pone.0218075 (2019).
90 Irish, A. K., Erickson, C. M., Wahls, T. L., Snetselaar, L. G. & Darling, W. G. Randomized control trial evaluation of a modified Paleolithic dietary intervention in the treatment of relapsing-remitting multiple sclerosis: a pilot study. *Degener Neurol Neuromuscul Dis* **7**, 1-18, doi:10.2147/DNND.S116949 (2017).
91 Lee, J. E. *et al.* A Multimodal, Nonpharmacologic Intervention Improves Mood and Cognitive Function in People with Multiple Sclerosis. *J Am Coll Nutr* **36**, 150-168, doi:10.1080/07315724.2016.1255160 (2017).

92 Wahls, T. L., Chenard, C. A. & Snetselaar, L. G. Review of Two Popular Eating Plans within the Multiple Sclerosis Community: Low Saturated Fat and Modified Paleolithic. *Nutrients* **11**, doi:10.3390/nu11020352 (2019).
93 Wahls, T. L. *et al.* Impact of the Swank and Wahls elimination dietary interventions on fatigue and quality of life in relapsing-remitting multiple sclerosis: The WAVES randomized parallel-arm clinical trial. *Mult Scler J Exp Transl Clin* **7**, 20552173211035399, doi:10.1177/20552173211035399 (2021).
94 Bjornevik, K., Chitnis, T., Ascherio, A. & Munger, K. L. Polyunsaturated fatty acids and the risk of multiple sclerosis. *Multiple sclerosis* **23**, 1830-1838, doi:10.1177/1352458517691150 (2017).
95 Penkert, H. *et al.* Proteomic and lipidomic profiling of demyelinating lesions identifies fatty acids as modulators in lesion recovery. *Cell Rep* **37**, 109898, doi:10.1016/j.celrep.2021.109898 (2021).
96 Poisson, L. M. *et al.* Untargeted Plasma Metabolomics Identifies Endogenous Metabolite with Drug-like Properties in Chronic Animal Model of Multiple Sclerosis. *J Biol Chem* **290**, 30697-30712, doi:10.1074/jbc.M115.679068 (2015).
97 Kooij, G. *et al.* Specialized pro-resolving lipid mediators are differentially altered in peripheral blood of patients with multiple sclerosis and attenuate monocyte and blood-brain barrier dysfunction. *Haematologica* **105**, 2056-2070, doi:10.3324/haematol.2019.219519 (2020).
98 Jelinek, G. A. *et al.* Association of fish consumption and Omega 3 supplementation with quality of life, disability and disease activity in an international cohort of people with multiple sclerosis. *Int J Neurosci* **123**, 792-800, doi:10.3109/00207454.2013.803104 (2013).
99 Matveeva, O. *et al.* Western lifestyle and immunopathology of multiple sclerosis. *Ann N Y Acad Sci* **1417**, 71-86, doi:10.1111/nyas.13583 (2018).
100 Rumble, J. M. *et al.* Neutrophil-related factors as biomarkers in EAE and MS. *J Exp Med* **212**, 23-35, doi:10.1084/jem.20141015 (2015).
101 Aube, B. *et al.* Neutrophils mediate blood-spinal cord barrier disruption in demyelinating neuroinflammatory diseases. *J Immunol* **193**, 2438-2454, doi:10.4049/jimmunol.1400401 (2014).
102 Jiang, W. *et al.* Infiltration of CCR2+Ly6Chigh Proinflammatory Monocytes and Neutrophils into the Central Nervous System Is Modulated by Nicotinic Acetylcholine Receptors in a Model of Multiple Sclerosis. *J Immunol* **196**, 2095-2108, doi:10.4049/jimmunol.1501613 (2016).
103 Levesque, S. A. *et al.* Myeloid cell transmigration across the CNS vasculature triggers IL-1beta-driven neuroinflammation during autoimmune encephalomyelitis in mice. *J Exp Med* **213**, 929-949, doi:10.1084/jem.20151437 (2016).
104 Steinbach, K., Piedavent, M., Bauer, S., Neumann, J. T. & Friese, M. A. Neutrophils amplify autoimmune central nervous system infiltrates by maturing local APCs. *J Immunol* **191**, 4531-4539, doi:10.4049/jimmunol.1202613 (2013).
105 Yan, Z. *et al.* Deficiency of Socs3 leads to brain-targeted EAE via enhanced neutrophil activation and ROS production. *JCI Insight* **5**, doi:10.1172/jci.insight.126520 (2019).
106 Openshaw, H. *et al.* Multiple sclerosis flares associated with recombinant granulocyte colony-stimulating factor. *Neurology* **54**, 2147-2150, doi:10.1212/wnl.54.11.2147 (2000).
107 Rust, H., Kuhle, J., Kappos, L. & Derfuss, T. Severe exacerbation of relapsing-remitting multiple sclerosis after G-CSF therapy. *Neurology(R) neuroimmunology & neuroinflammation* **3**, e215, doi:10.1212/NXI.0000000000000215 (2016).
108 Ghafouri-Fard, S., Honarmand, K. & Taheri, M. A comprehensive review on the role of chemokines in the pathogenesis of multiple sclerosis. *Metab Brain Dis* **36**, 375-406, doi:10.1007/s11011-020-00648-6 (2021).
109 Tsutsui, M. *et al.* TRPM2 Exacerbates Central Nervous System Inflammation in Experimental Autoimmune Encephalomyelitis by Increasing Production of CXCL2 Chemokines. *J Neurosci* **38**, 8484-8495, doi:10.1523/JNEUROSCI.2203-17.2018 (2018).
110 Bligh, E. G. & Dyer, W. J. A rapid method of total lipid extraction and purification. *Can J Biochem Physiol* **37**, 911-917, doi:10.1139/o59-099 (1959).
111 Li, F. *et al.* DHA does not protect ELOVL4 transgenic mice from retinal degeneration. *Mol Vis* **15**, 1185-1193 (2009).
112 Agbaga, M. P. *et al.* Differential composition of DHA and very-long-chain PUFAs in rod and cone photoreceptors. *J Lipid Res* **59**, 1586-1596, doi:10.1194/jlr.M082495 (2018).
113 Yu, M. *et al.* ELOVL4 protein preferentially elongates 20:5n3 to very long chain PUFAs over 20:4n6 and 22:6n3. *J Lipid Res* **53**, 494-504, doi:10.1194/jlr.M021386 (2012).

114 Axtell, R. C. *et al.* T helper type 1 and 17 cells determine efficacy of interferon-beta in multiple sclerosis and experimental encephalomyelitis. *Nat Med* **16**, 406-412, doi:10.1038/nm.2110 (2010).
115 Laird, N. M. & Ware, J. H. Random-effects models for longitudinal data. *Biometrics* **38**, 963-974 (1982).
116 Lindstrom, M. L. & Bates, D. M. Nonlinear mixed effects models for repeated measures data. *Biometrics* **46**, 673-687 (1990).

ACKNOWLEDGEMENTS

Research reported in this publication was in part supported by a Presbyterian Health Foundation Collaborative Sciences Grant to SMP and SK and in part by the National Eye Institute of the National Institutes of Health under Award Numbers R01EY033782 and R21EY026684. The content is solely the responsibility of the authors and does not necessarily represent the official views of the National Institutes of Health. We are grateful to members of the Plafker, Axtell, and Kovats laboratories at OMRF and the Agbaga lab at DMEI for helpful input. We thank Drs. Joel and Carla Guthridge for assistance with the multiplex cytokine studies. KZJ is grateful for the support of an OMRF pre-doctoral fellowship endowed by the Barrett Scholarship Fund. We also acknowledge unrestricted grant support from Research to Prevent Blindness and P30EY021725 to the Dean McGee Eye Institute for support of the Lipidomics core.

AUTHOR CONTRIBUTIONS

KZJ: experimental design, acquisition and analysis of data, writing and editing. **DAW:** acquisition and analysis of data, editing. **KSP:** acquisition and analysis of data, editing. **SK:** acquisition and analysis of data, editing. **CG:** statistical analyses, editing. **RSB:** acquisition and analysis of data, editing. **MT:** acquisition and analysis of data, editing. **MPA:** acquisition and analysis of data, editing. **SMP:** experimental design, writing and editing.

DATA AVAILABILITY

The data generated and analyzed for this study are included in this published article and its Supplementary information files.

COMPETING INTERESTS STATEMENT

The authors declare no competing interests.

FIGURE LEGENDS

Figure 1. The WFKD is non-obesogenic, stabilizes blood glucose, and increases circulating ketones. **(A)** Outline of the experimental approach. Mice were put on a WFKD or CD for 2 weeks prior to MOG_{35-55} immunization to acclimate and maintained on their respective diets for the duration of the experiment. Motor scores and visual acuity were tracked daily, and blood draws (red drop symbol) for glucose and ketone levels were taken at days -14, 0, and 21 dpi. Tissues and plasma were harvested 3 weeks post immunization. **(B)** Macromolecular compositions of diets. The sources of carbohydrate in the CD are corn starch, maltodextrin, sucrose, and fiber in the form of cellulose. The WFKD contains only cellulose. The fat content of the WFKD is derived from MCTs (C8 and C10), flaxseed oil, and canola oil. **(C-E)** Graphs of body weights (C), blood glucose levels (D), and blood ketones (E) as a function of days before and after MOG_{35-55} immunization. For graphs, blue and green traces show female and male mice on WFKD, respectively. Red and purple traces show female and male mice on CD, respectively. N=10-17 mice/sex. Asterisks denote statistical significance ($p<0.05$) by multiple t-test. Whisker-bar standard deviations and p-values for differences between curves in C were computed with mixed linear model implementation of lme function, nlme R package. * $P<0.05$, ** $P<0.01$, *** $P<0.001$, **** $P<0.0001$.

Figure 2. The WFKD ameliorates motor deficits in female and male mice. Daily motor scores of female mice **(A)** and male mice **(B)** on the indicated diets. For both graphs, blue and green traces show female and male mice on WFKD, respectively, with red and purple traces showing female and male mice on CD, respectively. N=10-17 mice/sex. Whisker-bar standard deviations and p-values for differences between curves were computed with mixed linear model implementation of lme function, nlme R package. Asterisks denote statistical significance ($p<0.05$).

Figure 3. The WFKD prevents visual acuity deficits by sparing retinal ganglion cells in female and male mice. **(A)** OKT measurements of visual acuity of the more affected (MA; top graph) and less affected (LA; bottom graph) eyes in female mice on the indicated diets. n=14-17 mice/diet. **(B)** Same as (A) for male mice. n=10-12 mice/diet. **(C)** Representative photomicrographs of $Brn3A^+$ RGCs in the central, medial, and peripheral retinas of mice as a function of diet. Examples are shown for both the more affected (MA) and the

less affected (LA) eyes. **(D)** Graph of Brn3A$^+$ RGC cell counts in central, medial, and peripheral retinas of female and male mice combined as a function of diet. WFKD (green bars) and CD (yellow bars). **(E)** Graph of Brn3A$^+$ RGC cell counts in central, medial, and peripheral retinas as a function of sex and diet. Whisker-bar standard deviations and p-values for differences between curves in A and B were computed with mixed linear model implementation of lme function, nlme R package. Mann-Whitney test was performed for (D) and (E). Asterisks in all graphs denote statistical significance ($p<0.05$) and 'ns' denotes not significant. * $P<0.05$, ** $P<0.01$, *** $P<0.001$, **** $P<0.0001$.

Figure 4. The WFKD preserves oligodendrocytes on the optic nerve and reduces infiltrating macrophages and T cells. (A) Representative photomicrographs of paraffin-embedded optic nerve sections stained for the indicated markers (CNPase, Iba1, and CD3) from healthy (non-EAE) mice as well as males and females subjected to EAE and consuming the indicated diets. Sections spanning the entire length of the optic nerve were labeled with each marker and quantified. Size bar corresponds to 100 μm. **(B-D)** Mean values and 95% confidence intervals for CNPase (B), Iba1 (C), and CD3 (D) labeling of optic nerve sections. Data shown for females and males separately as well as combined. Whisker bars depict 95% confidence intervals for each variable and horizontal bars with accompanying p-values above the bars indicate statistical significance. **(E)** Principal components (PC) biplot to summarize, in 2d projection, the similarities among the mice groups and their relationships to the 5 measured scores (i.e., motor, OKT, CNPase, Iba1, CD3). The dots on the graph are samples, colored according to their phenotype group, with the measured variables shown as arrows. Arrow coordinates on the two axes show each variable contributing loading on the first two principal components. Multidimensional 95% confidence regions for each mouse group, projected in 2d, are shown as ellipses. All data acquired from $n\geq 4$ mice/sex/diet. The graph below the PC biplot makes explicit, for the five markers, the difference between the two clusters of mice (Healthy+WFKD versus CD) separated by the first principal component. Whisker bars depicting 95% confidence intervals are shown for each variable both in Healthy+WFKD mice and in CD mice with the p-values assessing the significance of their differences marked on the graph.

Figure 5. The WFKD increases plasma ω3 fatty acid content. (A) List of fatty acids analyzed. The omega designations, the common names, and the systematic names are provided for each lipid. **(B-D)** Log-scale graphs depicting nmols of individual fatty acids per mg of protein in the plasma that are statistically significantly different (*$p \leq 0.05$, **$p<0.01$, ***$p<0.001$, ****$p<0.0001$ as determined by Mann-Whitney test, with Bonferroni correction) between EAE mice fed the WFKD versus the CD. Graphs represent females (**B**), males (**C**), and the sexes combined (**D**). The complete set of fatty acid measurements is provided in Supplemental Figs. 1 C-E. In (**B-D**), the ratio of arachidonic acid (AA; 20:4n6) to (EPA +DHA) (20:5n3 + 22:6n3) is included as a proxy of systemic inflammation. Note: all graphs use log scale with data derived from $n \geq 3$ mice per diet for each sex.

Figure 6. The WFKD reduces G-CSF, CXCL2, and other markers of inflammation. (A-F) Graphs showing concentrations of the indicated cytokines and chemokines in the plasma 21 dpi of female and male EAE mice consuming either a CD (orange) or the WFKD (blue). Data derived from $n \geq 4$-8 mice per diet for each sex. Statistical significance was determined by Mann-Whitney test with ns indicating not significant. * $p<0.05$, ** $p<0.01$, *** $p<0.001$, **** $p<0.0001$. The complete set of cytokine and chemokine measurements is provided in Supplemental Figs. 2A-D. With the exception of the 6 factors shown in this figure, the remaining cytokines and chemokines either were not statistically significantly different between diets or the number of samples below the detection limit of the ELISA precluded statistical comparisons.

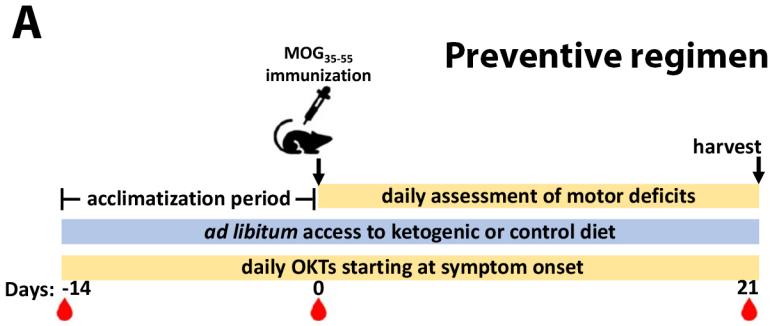

B

	WFKD	CD
Kcal/g	4.7	3.6
Protein [% kcal]	22.4	20.4
Carbohydrate [% kcal]	0.5	69.3
Fat [% kcal]	77.1	10.4
Select ingredients	[g/kg]	[g/kg]
Corn starch	0	369.29
Maltodextrin	0	100.0
Sucrose	0	200.0
Fiber (cellulose)	245.31	40.0
Medium Chain Triglycerides (MCTs)	270	0
Flaxseed oil	70.0	21.0
Canola oil	60.0	19.0

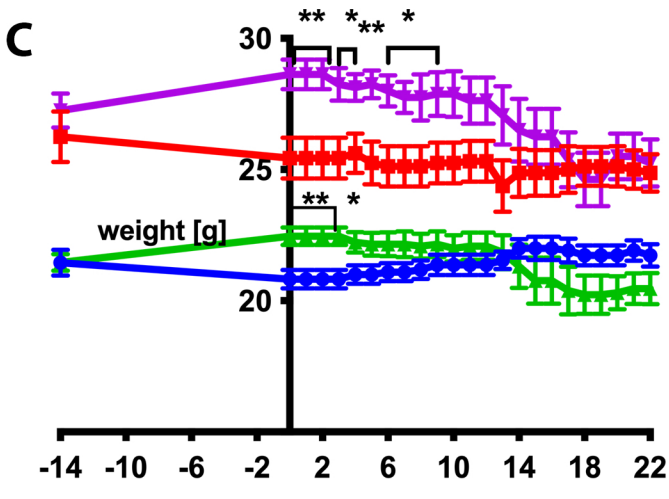

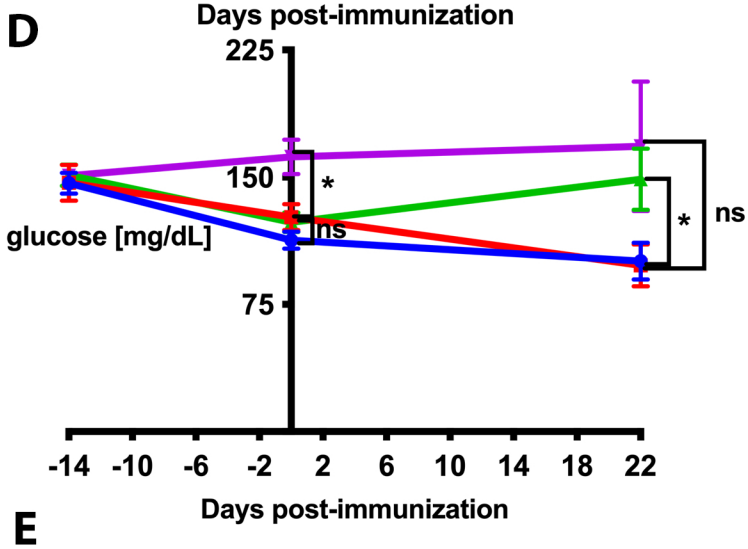

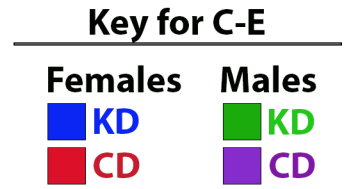

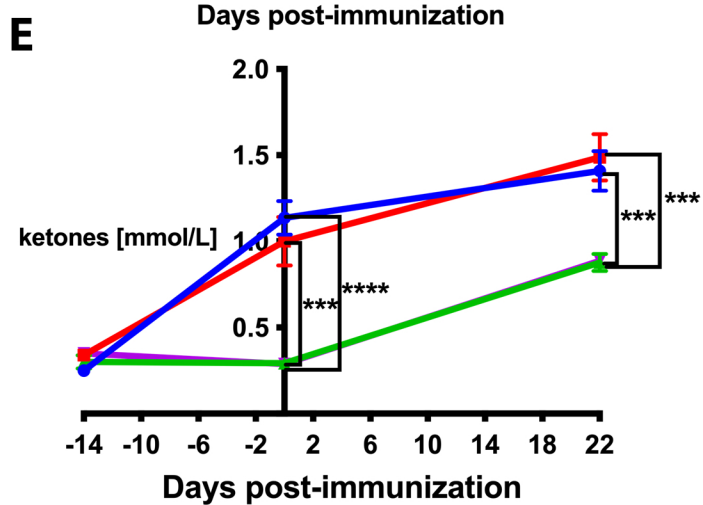

Figure 1

Figure 2

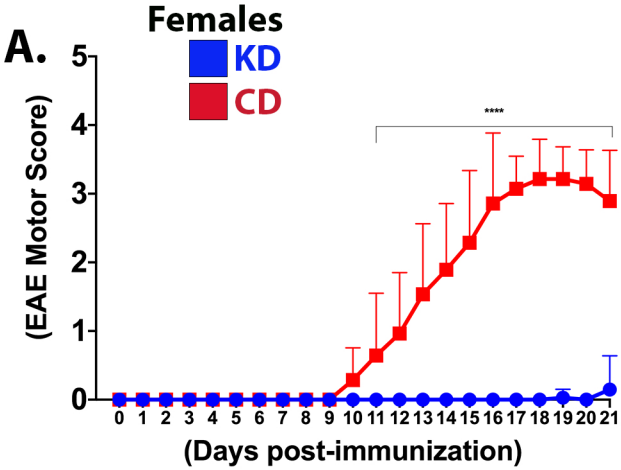
A.
Females
KD
CD
****
(EAE Motor Score)
0
1
2
3
4
5
0 1 2 3 4 5 6 7 8 9 10 11 12 13 14 15 16 17 18 19 20 21
(Days post-immunization)

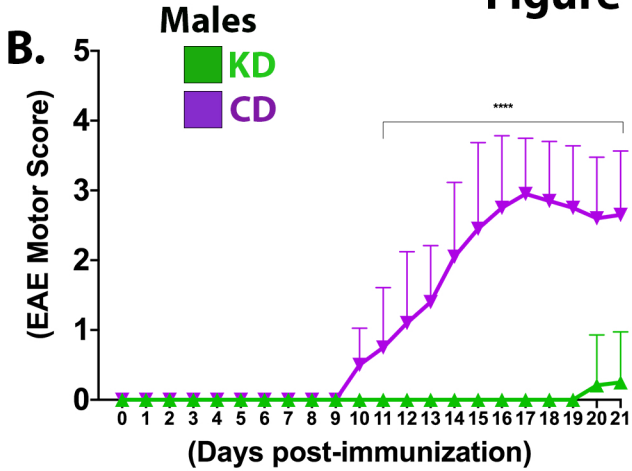
B.
Males
KD
CD
****
(EAE Motor Score)
0
1
2
3
4
5
0 1 2 3 4 5 6 7 8 9 10 11 12 13 14 15 16 17 18 19 20 21
(Days post-immunization)

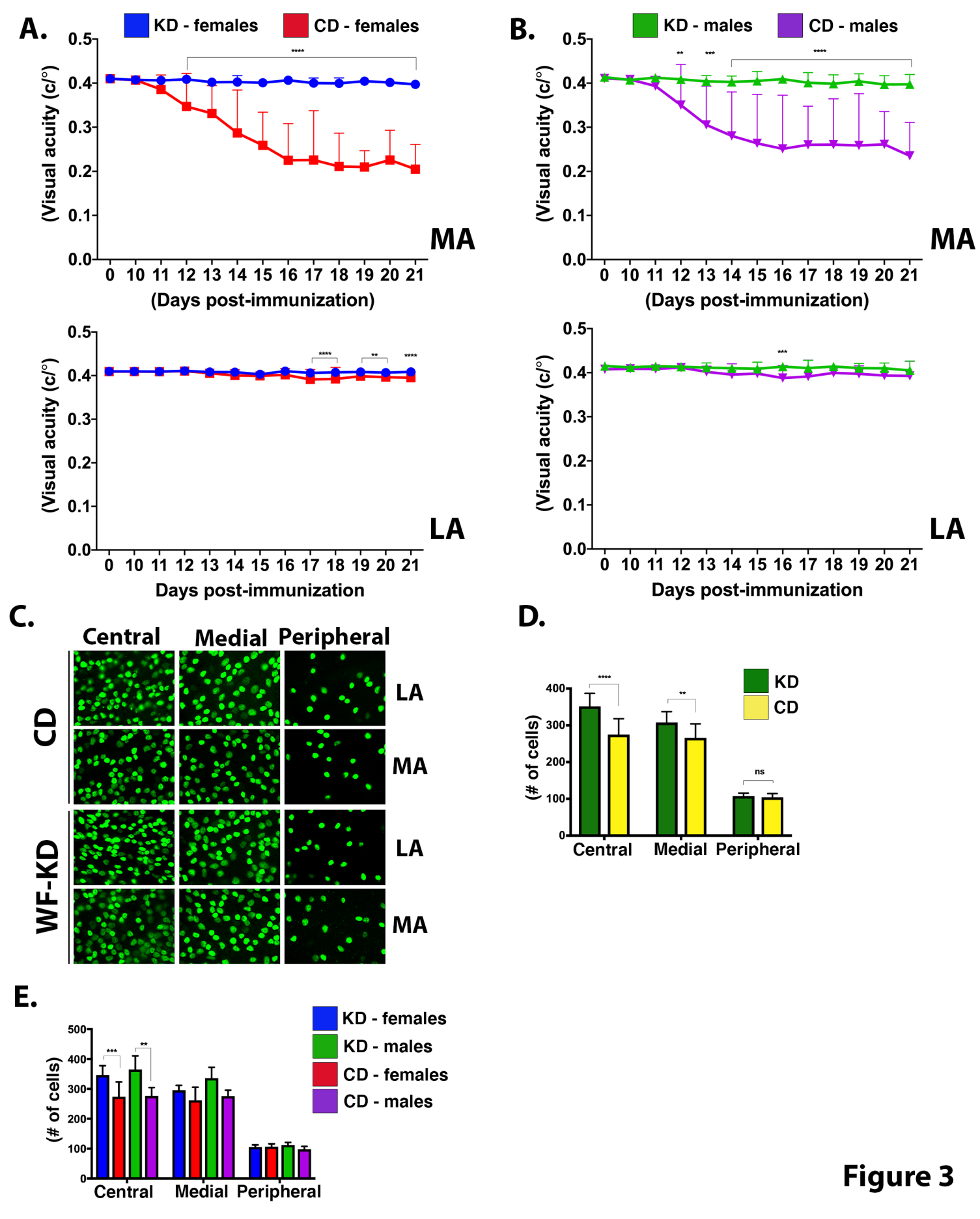
A.
KD - females
CD - females
(Visual acuity (c/°))
(Days post-immunization)
MA
LA
B.
KD - males
CD - males
C.
Central
Medial
Peripheral
CD
WF-KD
D.
KD
CD
(# of cells)
ns
E.
KD - females
KD - males
CD - females
CD - males

Figure 3

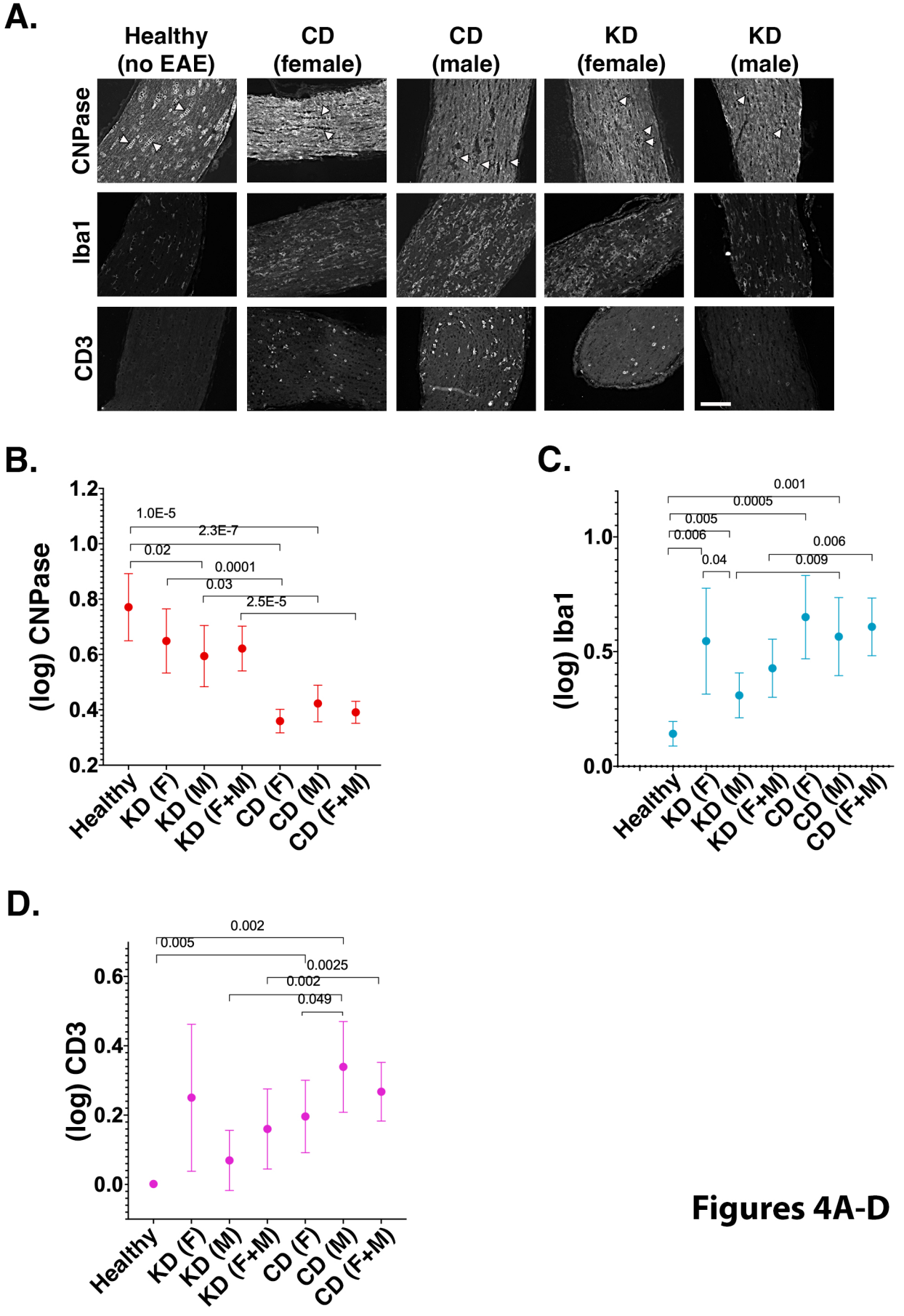
A.
Healthy (no EAE)
CD (female)
CD (male)
KD (female)
KD (male)
CNPase
Iba1
CD3
B.
(log) CNPase
1.2
1.0
0.8
0.6
0.4
0.2
1.0E-5
2.3E-7
0.02
0.0001
0.03
2.5E-5
Healthy
KD (F)
KD (M)
KD (F+M)
CD (F)
CD (M)
CD (F+M)
C.
(log) Iba1
1.0
0.5
0.0
0.001
0.0005
0.005
0.006
0.006
0.04
0.009
Healthy
KD (F)
KD (M)
KD (F+M)
CD (F)
CD (M)
CD (F+M)
D.
(log) CD3
0.6
0.4
0.2
0.0
0.002
0.005
0.0025
0.002
0.049
Healthy
KD (F)
KD (M)
KD (F+M)
CD (F)
CD (M)
CD (F+M)

Figures 4A-D

E.

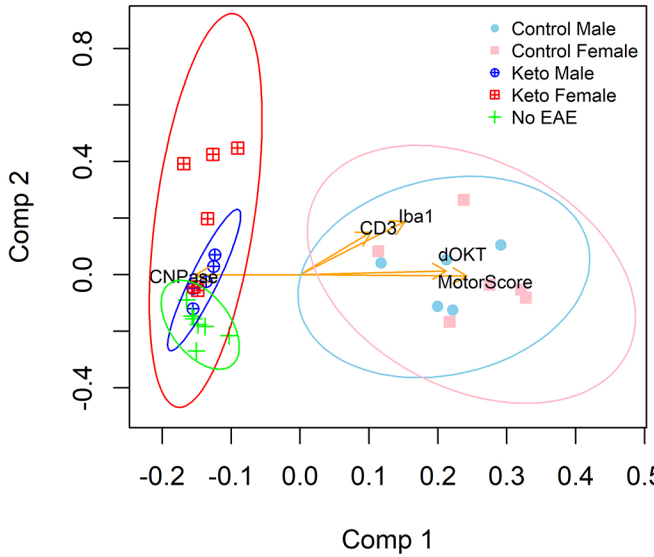
Control Male
Control Female
Keto Male
Keto Female
No EAE
Comp 2
Comp 1
0.8
0.4
0.0
-0.4
-0.2
-0.1
0.0
0.1
0.2
0.3
0.4
0.5
CD3
Iba1
dOKT
MotorScore
CNPase

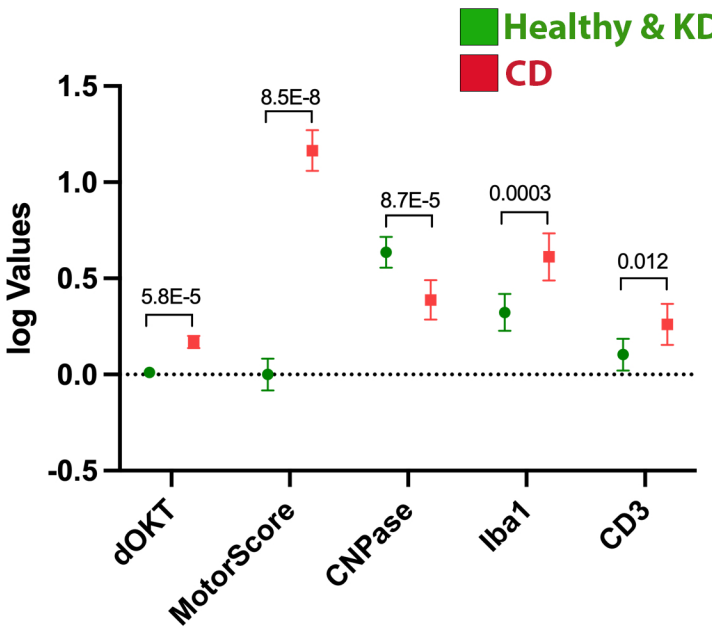
Healthy & KD
CD
log Values
1.5
1.0
0.5
0.0
-0.5
5.8E-5
8.5E-8
8.7E-5
0.0003
0.012
dOKT
MotorScore
CNPase
Iba1
CD3

Figure 4E

Figure 5

A.

Lipid	Common name	Systematic name
14:0	Myristic acid	Tetradecanoic acid
16:0	Palmitic acid	Hexadecanoic acid
16:1	Palmitoleic acid	hexadec-9-enoic acid
18:0	Stearic acid	Octadecanoic acid
18:1	Oleic acid	*Cis*-9-octadecenoic acid
18:2n6	Linoleic acid (LA)	*all-cis*-9,12-octadecadienoic acid
18:3n6	Gamma-linolenic acid (GLA)	*all-cis*-6,9,12-octadecatrienoic acid
18:3n3	Alpha-linolenic acid (ALA)	*all-cis*-9,12,15-octadecatrienoic acid
20:0	Arachidic acid	Eicosanoic acid
20:1	Eicosenoic acid	*cis*-11-eicosenoic acid
20:3n9	Eicosatrienoic acid	(5Z,8Z,11Z)-Icosa-5,8,11-trienoic acid
20:4n3	Eicosatetraenoic acid (ETA)	*all-cis*-8,11,14,17-eicosatetraenoic acid
20:5n3	Eicosapentaenoic acid (EPA)	*all-cis*-5,8,11,14,17-eicosapentaenoic acid
20:2n6	Eicosadienoic acid	*all-cis*-11,14-eicosadienoic acid
20:3n6	Dihomo-gamma-linolenic acid (DGLA)	*all-cis*-8,11,14,-eicosatrienoic acid
20:4n6	Arachidonic acid (AA)	*all-cis*-5,8,11,14,-eicosatetraenoic acid
22:0	Behenic acid	Docosanoic acid
22:1	Erucic acid	*cis*-13-docosenoic acid
22:5n3	Docosapentaenoic acid (DPA)	*all-cis*-7,10,13,16,19-docosapentaenoic acid
22:6n3	Docosahexaenoic acid (DHA)	*all-cis*-4,7,10,13,16,19-docosahexaenoic acid

B.

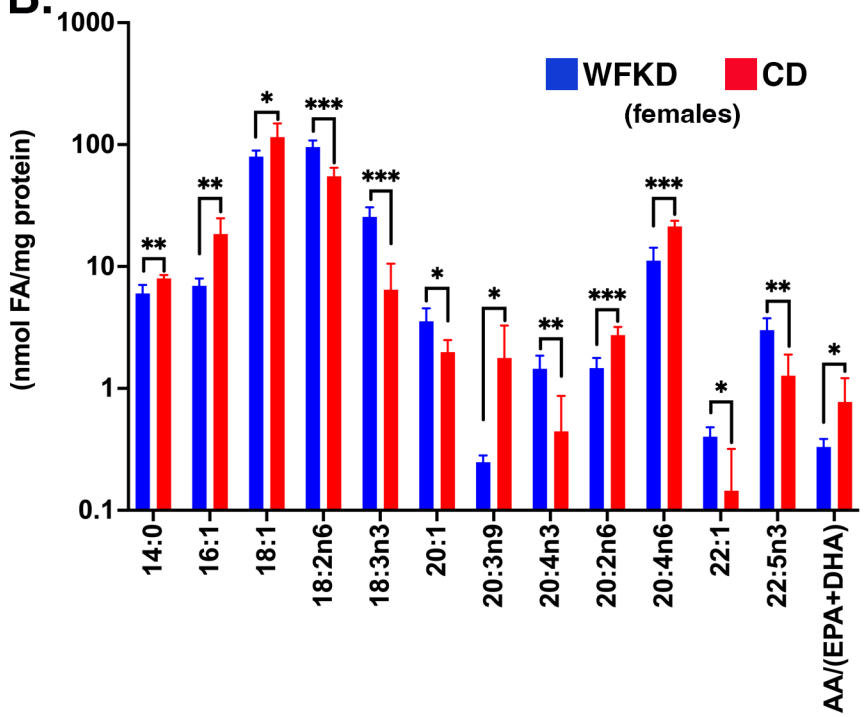

C.

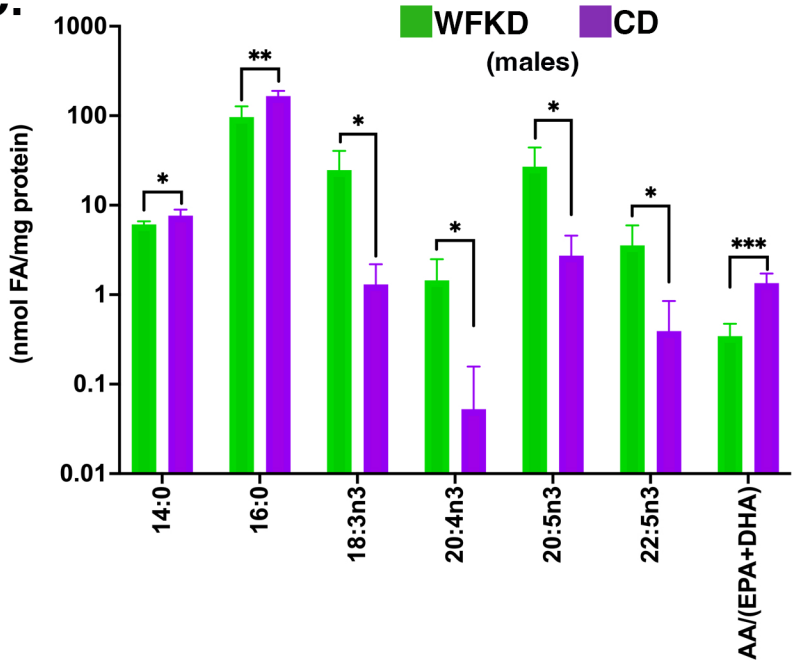

D.

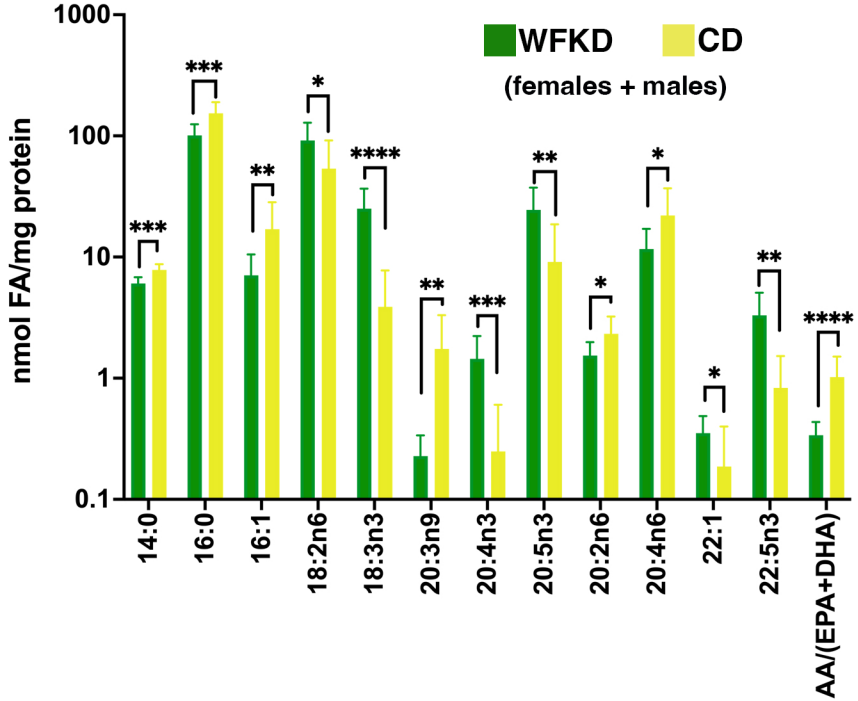

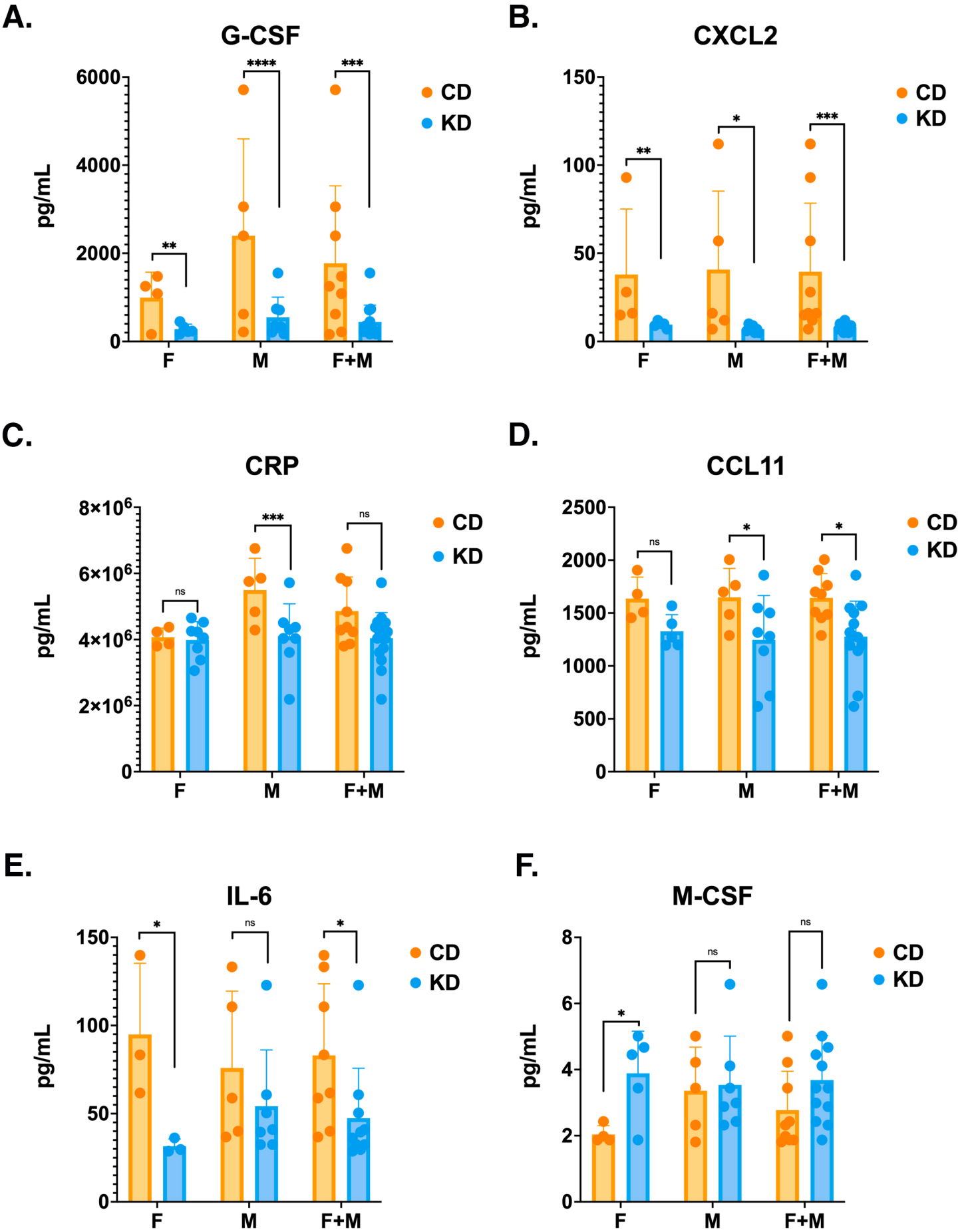
A.
G-CSF
pg/mL
6000
4000
2000
0
**
****
***
F
M
F+M
CD
KD
B.
CXCL2
pg/mL
150
100
50
0
**
*
***
F
M
F+M
CD
KD
C.
CRP
pg/mL
8×10^6
6×10^6
4×10^6
2×10^6
0
ns
***
ns
F
M
F+M
CD
KD
D.
CCL11
pg/mL
2500
2000
1500
1000
500
0
ns
*
*
F
M
F+M
CD
KD
E.
IL-6
pg/mL
150
100
50
0
*
ns
*
F
M
F+M
CD
KD
F.
M-CSF
pg/mL
8
6
4
2
0
*
ns
ns
F
M
F+M
CD
KD

Figure 6